FRAUNHOFER INSTITUTE FOR WIND ENERGY SYSTEMS IWES

IWES WIND TURBINE IWT-7.5-164

– REV 4 –

This report has to be cited in the following form:
Popko W., Thomas P., Sevinc A., Rosemeier M., Bätge M., Braun R., Meng F., Horte D., Balzani C., Bleich O., Daniele E., Stoevesandt B., Wentingmann M., Polman J. D., Leimeister M., Schümann B., Reuter A. (2018). *IWES Wind Turbine IWT-7.5-164 Rev 4*. Fraunhofer Institute for Wind Energy Systems IWES. Bremerhaven. https://doi.org/10.24406/IWES-N-518562

Fraunhofer Institute for Wind Energy Systems IWES
Am Seedeich 45
27572 Bremerhaven
Germany

+49 (0) 471 14290-100
iweswindturbine@iwes.fraunhofer.de
www.iwes.fraunhofer.de

IWT Rev	Issue date	Author	Changelog
0	2013-12-30	Alper Sevinc[1,2], Malo Rosemeier[1], Moritz Bätge[1,2], Roman Braun[1], Fanzhong Meng[1], Martin Shan[1], Daria Horte[2], Claudio Balzani[2], Andreas Reuter[1,2]	Initial document
1	2014-08-11	Alper Sevinc[1,2], Malo Rosemeier[1], Moritz Bätge[1,2], Roman Braun[1], Fanzhong Meng[1], Martin Shan[1], Daria Horte[2], Claudio Balzani[2], Andreas Reuter[1,2]	Controller update, blade design update
2	2015-03-11	Alper Sevinc[1,2], Malo Rosemeier[1], Moritz Bätge[1,2], Roman Braun[1], Fanzhong Meng[1], Martin Shan[1], Daria Horte[2], Claudio Balzani[2], Andreas Reuter[1,2]	Included controller specification, new structural blade data
2.5	2016-08-15	Oliver Bleich[1], Fanzhong Meng[1], Elia Daniele[1], Philipp Thomas[1], Wojciech Popko[1]	Corrected hub, nacelle, and blade mass according to BECAS HAWC2 output Acknowledgments and nomenclature Coordinate system description Updated figures with updated simulation models Enhanced image quality Updated Campbell diagram and included Eigenfrequencies for rotor blades and tower Add drawing of nacelle geometry Enhanced description of the turbine controller and control parameter tuning Add power production simulation time series Add airfoil data for an angle of attack range of -180° to 180°
2.5	2017-06-21	Philipp Thomas[1]	Change Acknowledgements, Authors, and changelog
4	2018-03-05	Wojciech Popko[1]	"Nomenclature" section – added units Reorganized sub-sections in Chapter 3 Updated and corrected: blade structural and geometrical properties; blade length and mass; hub height; mass and mass moment of inertia of nacelle, hub, and generator; RNA geometry and center of gravity positions "Pitch system" section – Removed
4	2018-07-13	Mareike Leimeister[1]	"Matlab Simulink" section – New section describing S-function model
4	2018-07-17	Elia Daniele[2]	Aerodynamic properties updated Aerodynamic design description
4	2018-08-31	Wojciech Popko[1]	"Lists of figures and tables" – Removed "Nomenclature" section – Updated and cleaned "Coordinate systems" section – Entirely new figures and descriptions "RNA" section – Rewritten text, corrected definitions, new figures "Blade" section – Rewritten text, corrected definitions, new figures "Eigenfrequencies and Campbell diagram"– Entirely rewritten, new figures "Bibliography" section – Updated, corrected, cleaned, and added hyperlinks "Appendix B" – Removed polar figures "Appendix C" – New section with the nacelle and spinner housing Included hyperlinks to Excel files with blade and support structure design data
4	2018-08-31	Mareike Leimeister[1]	Updated properties table for TANDEM offshore wind turbine Included Campbell diagram for TANDEM offshore wind turbine "Matlab Simulink" section – Added "Requirements.." subsection Updated references to tables in the section on the S-function
4	2018-12-10	Wojciech Popko[1]	"Coordinate systems" section – updated and rewritten Updates –> all figures with blade properties, tip speed ratio definition Document formatting and comments from the group. Controller information updated Included DOI number

Authors

Editors of Revision 4
Wojciech Popko[1], Philipp Thomas[1]

General turbine concept
Andreas Reuter[1,2], Claudio Balzani[2], Alper Sevinc[1,2], Bernhard Stoevesandt[1]

Blade structural and geometrical design
Malo Rosemeier[1], Moritz Bätge[1,2], Roman Braun[1], Claudio Balzani[2], Michael Wentingmann[2], Jelmer Derk Polman[2]

Airfoil polars
Elia Daniele[1]

Nacelle and spinner design
Alper Sevinc[1,2]

Onshore support structure design
Alper Sevinc[1,2], Daria Horte[2]

Offshore support structures design
Björn Schümann[3]

Bladed V4.9 models
Wojciech Popko[1]

HAWC2 model
Fanzhong Meng[1], Wojciech Popko[1], Oliver Bleich[1]

MATLAB Simulink S-function model
Mareike Leimeister[1], Philipp Thomas[1]

[1] Fraunhofer Institute for Wind Energy Systems IWES
Am Seedeich 45
27572 Bremerhaven
Germany

[2] Leibniz University Hannover
Institute for Wind Energy Systems
Appelstraße 9A
30167 Hannover
Germany

[3] Ramboll GmbH
Stadtdeich 7
20097 Hamburg
Germany

Content

Acknowledgments

The present work was funded within the framework of the joint projects Smart Blades (FKZ 0325601A/B/C/D) and SmartBlades 2 (FKZ 0324032A/B/C/D).

The monopile offshore support structures were designed by Ramboll within the projects: SeaLOWT ("Impact of Sea Ice Loads on Global Dynamics of Offshore Wind Turbines", FKZ 0324022B) and TANDEM ("Towards an Advanced Design of Large Monopiles", FKZ 0325841B).

The Smart Blades, SmartBlades 2, SeaLOWT and TANDEM projects were funded by the German Federal Ministry for Economic Affairs and Energy (BMWi) on the basis of a decision by the German Federal Parliament.

Supported by:

Federal Ministry
for Economic Affairs
and Energy

on the basis of a decision
by the German Bundestag

Nomenclature

Abbreviation	Description
BECAS	BEam Cross-section Analysis Software
BEM	Blade Element Momentum
CG	Center of Gravity
DLL	Dynamic Link Library
DOF	Degree of Freedom
DTU	Danmarks Tekniske Universitet
HAWC2	Horizontal Axis Wind turbine simulation Code 2nd generation
IEC	International Electrotechnical Commission
MoWiT	Modelica for Wind Turbines
MSL	Mean Sea Level
NREL	National Renewable Energy Laboratory
RFOIL	Radial XFOIL
RNA	Rotor-Nacelle Assembly
XFOIL	Subsonic Airfoil Development System

Symbol	Unit	Description
A	m²	Cross-sectional area of the airfoil
$C_{1/2}$	-	Center of the local airfoil coordinate system
C_{a}	-	Aerodynamic drag coefficient for nacelle housing
$C_{\mathrm{P,max}}$	-	Maximum power coefficient
C_{P}	-	Power coefficient
C_{Q}	-	Torque coefficient
C_{T}	-	Thrust coefficient
D_{R}	m	Rotor diameter (coned blades)
D_{RN}	m	Nominal rotor diameter (unconed blades)
E	N/m²	Young's modulus
G	N/m²	Shear modulus
I	kg m^2	Moment of inertia
I_{x}	m^4	Area moment of inertia about principal bending x_{ec}-axis
I_{y}	m^4	Area moment of inertia about principal bending y_{ec}-axis
K	m^4/rad	Torsional stiffness constant about the z_{ec}-axis. For a circular section, it is identical to the polar moment of inertia
P	kW	Generator electrical power including losses
P_{r}	kW	Generator rated electrical power including losses
Q	kNm	Generator torque
R_{H}	m	Hub radius
T	kN	Rotor thrust force
T_{r}	kN	Rated rotor thrust force at the rated wind speed
V	m/s	Wind speed at the hub height

V_{in}	m/s	Cut-in wind speed at the hub height, at which wind turbine starts to generate power
V_{out}	m/s	Cut-out wind speed at the hub height, at which wind turbine is shut down
V_{r}	m/s	Rated wind speed at the hub height, at which turbine reaches rated electrical power
$V_{\mathrm{tip,r}}$	m/s	Rated blade tip speed
c	m	Chord length, the distance between the leading and trailing edge
$e_{\mathrm{pb,tip}}$	m	Pre-bend distance at the blade tip, measured along y_{b}-axis
e_{pb}	m	Pre-bend distance along y_{b}-axis, measured from the pitch z_{b}-axis to the chord line. (This definition is correct, as long the blade pre-sweep is zero)
k_{x}	-	Shear factor in principal bending x_{ec}-direction
k_{y}	-	Shear factor in principal bending y_{ec}-direction
l_{B}	m	Blade length along the pitch z_{b}-axis
l_{BC}	m	Arc length of the blade, measured along the blade centerline
m	kg/m	Mass per unit length
m_{B}	t	Single blade mass
m_{RNA}	t	Mass of rotor-nacelle assembly
r	m	Curved length distance from the center of the blade root coordinate system crossing the $C_{1/2}$-centers of the local airfoil coordinate systems
r_{ix}	m	Radius of gyration w.r.t. rotation about principal bending x_{ec}-axis
r_{iy}	m	Radius of gyration w.r.t. rotation about principal bending y_{ec}-axis
t	m	The largest distance between the suction side and the pressure side on a line perpendicular to the camber line
x	m	Coordinate in the global coordinate system, the axis points downwind
x_{b}	m	Coordinate in the blade root coordinate system
x_{e}	m	Distance from the $C_{1/2}$-center to the elastic center, measured along the x_{c2}-axis
x_{m}	m	Distance from the $C_{1/2}$-center to the mass center, measured along the x_{c2}-axis
x_{mb}	m	Distance from the center of the blade root coordinate system to the $C_{1/2}$-center of the local airfoil coordinate system, measured along the x_{b}-axis
x_{pa}	%	Distance from the airfoil leading edge to the pitch z_{b}-axis, divided by the chord length, measured along the chord x_{c2}-axis
x_{s}	m	Distance from the $C_{1/2}$-center to the shear center, measured along the x_{c2}-axis
x_{t}	m	Coordinate in the tower top coordinate system, the axis points downwind
y	m	Coordinate in the global coordinate system, the axis points to the side
y_{b}	m	Coordinate in the blade root coordinate system
y_{e}	m	Distance from the $C_{1/2}$-center to the elastic center, measured along the y_{c2}-axis
y_{m}	m	Distance from the $C_{1/2}$-center to the mass center, measured along the y_{c2}-axis
y_{mb}	m	Distance from the center of the blade root coordinate system to the $C_{1/2}$-center of the local airfoil coordinate system, measured along the y_{b}-axis
y_{s}	m	Distance from the $C_{1/2}$-center to the shear center, measured along the

		y_{c2}-axis
y_t	m	Coordinate in the tower top coordinate system, the axis points to the side
z	m	Coordinate in the global coordinate system, the axis points vertically upwards
z_b	m	Coordinate in the blade root coordinate system along the pitch axis
z_{mb}	m	Distance from the center of the blade root coordinate system to the $C_{1/2}$-center of the local airfoil coordinate system, measured along the pitch z_b-axis
z_t	m	Coordinate in the tower top coordinate system, the axis points vertically upwards
Ω	rpm	Rotor and generator rotational speed
Ω_{min}	rpm	Minimum rotational speed when the generator is put online
Ω_r	rpm	Rated rotor and generator rotational speed
η_{tot}	%	Total (combined mechanical and electrical) turbine efficiency
θ_{cone}	°	Blade cone angle in the upwind direction, measured between the rotor plane and the pitch z_b-axis
θ_p	°	Blade pitch angle around the pitch z_b-axis, positive in the clockwise direction
θ_{tilt}	°	Shaft tilt angle upwards from the horizontal plane
θ_{twist}	°	Local aerodynamic twist angle between the plane created by x_b- and z_b-axes of the blade root coordinate system, and the chord, positive in the upwind direction
θ_Z	°	Local structural twist angle between the x_{c2}-axis and the main principal bending x_{ec}-axis
λ	-	Blade tip speed ratio
λ_{max}	-	Blade tip speed ratio at which C_p reaches its maximum value
λ_r	-	Blade rated tip speed ratio, calculated as: $V_{tip,r}/V_r$
ψ_r	W/m²	Specific power per rotor-swept area

1 Introduction

Detailed wind turbine models for load simulations are essential for many research topics as they build the base for the verification and validation of most of the different disciplines in wind energy research. Turbine models, for example, the NREL 5-MW Offshore Baseline Turbine [1] or the DTU 10-MW Reference Wind Turbine [2], were developed in the last years and are used to contribute to wind turbine research especially in terms of further development of turbine design, controllers, and engineering methods on wind turbines.

A new state-of-the-art 7.5 MW turbine model was designed within the Smart Blades project funded by the German Federal Ministry for Economic Affairs and Energy. This turbine model has a specific design focus on the rotor blades.

This specification includes technical data to implement the numerical turbine model in a simulation environment and serves as a baseline for detailed component design and scientific research.

This report is part of the large package, which consists of a number of files with detailed definitions of various wind turbine components and aeroelastic models. The entire package can be downloaded from the Fraunhofer GitLab repository:

https://gitlab.cc-asp.fraunhofer.de/iwt/iwt-7.5-164

The folder structure of the provided repository is shown in Figure 1-1. Multiple files are hyperlinked to this report with the relative path links. **The relative hyperlinks in this report will only work if this report is opened from the following relative directory:**

`..\IWT-7.5-164\1 Report`

The onshore version of the turbine model described in this report, as it was developed in the Smart Blades project, is also named "SB-ReferenceTurbine" elsewhere (which is an abbreviation for "Smart Blades Reference Turbine"). For referencing in publications, the citation rule indicated on the front page has to be applied.

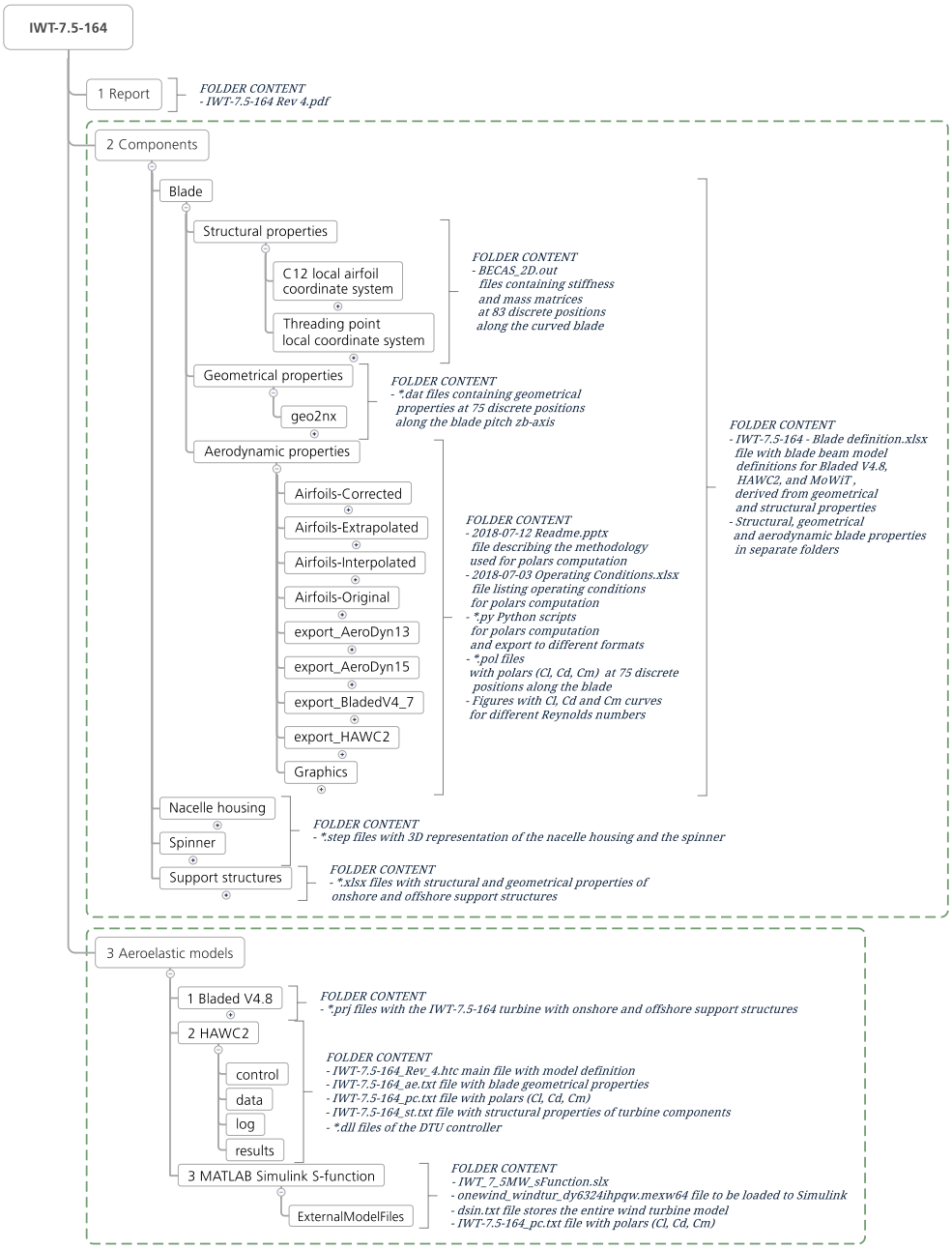

Figure 1-1: Folder structure and folder content

2
Coordinate systems

Five coordinate systems are defined for the model – the global coordinate system, the tower top coordinate system, the blade root coordinate system, the local airfoil coordinate system, and the local airfoil elastic coordinate system, respectively.

2.1
Global coordinate system

The global coordinate system is shown in Figure 2-1. It is a right hand Cartesian coordinate system. Its origin lays at the tower bottom where the horizontal plane crosses the tower centerline. The x-axis points downwind with respect to the main wind direction; the y-axis points to the side; the z-axis points vertically upwards.

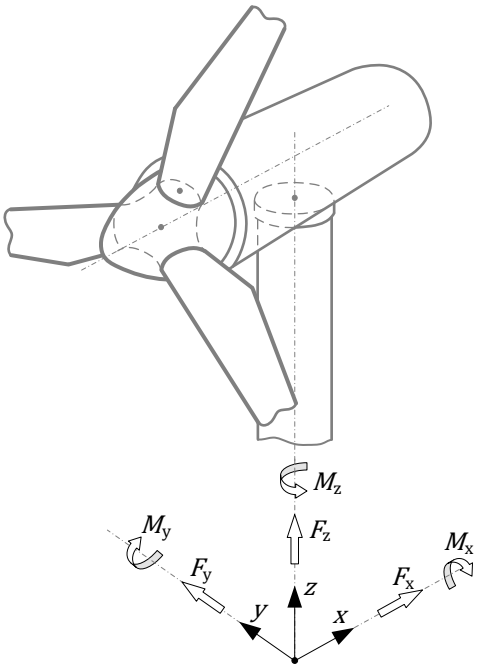

Figure 2-1: Global coordinate system – modified sketch from [3]

2.2 Tower top coordinate system

The tower top coordinate system is shown in Figure 2-2. Its origin is located at the point where the tower top horizontal plane crosses the vertical centerline of the tower. It is a right hand Cartesian coordinate system, where:

- The x_t-axis points downwind with respect to the main wind direction.
- The y_t-axis points to the side.
- The z_t-axis points vertically upwards.

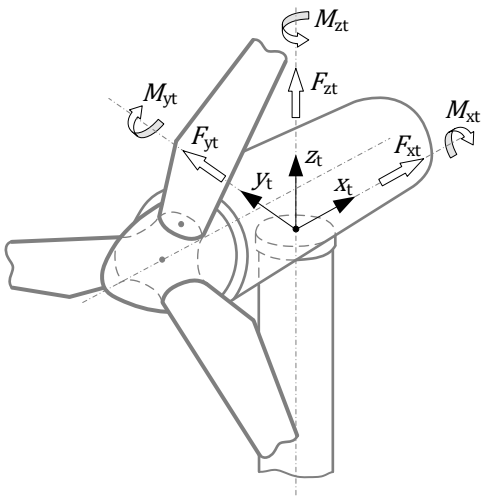

Figure 2-2: Tower top coordinate system – modified sketch from [3]

2.3 Blade root coordinate system

The blade root coordinate system is shown in Figure 2-3. It is a right hand Cartesian coordinate system, which:

- Is located at the center of the blade root plane, with the distance, R_{hub}, from the centerline of the main shaft.
- Is tilted with the shaft tilt angle, θ_{tilt}.
- Is coned with the rotor cone angle, θ_{cone}.
- Pitches in the clockwise direction, around the pitch z_{b}-axis, with the blade pitch angle, θ_{p}. This means that:
    - In case of $\theta_{\mathrm{p}} = 0°$, the x_{b}-axis is parallel to the rotor plane and points towards the rotational direction; the y_{b}-axis points downwind; the pitch z_{b}-axis points radially outwards.
    - In case of $\theta_{\mathrm{p}} = 90°$, the x_{b}-axis points upwind; the y_{b}-axis is parallel to the rotor plane and points towards the rotational direction; the pitch z_{b}-axis points radially outwards.
- Rotates with the rotor.

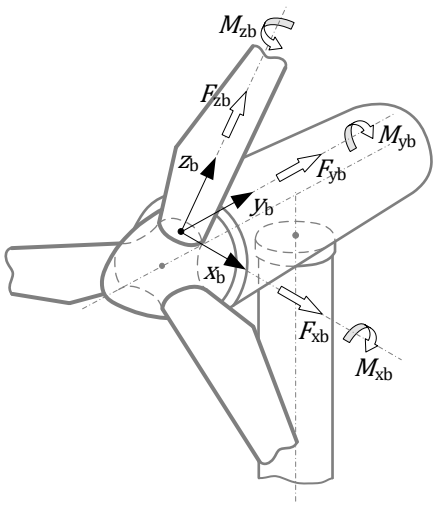

Figure 2-3: Blade root coordinate system for pitch angle of 0° – modified sketch from [3]

2.4 Local airfoil coordinate systems

The local airfoil coordinate systems are shown in Figure 2-4.

The origin (marked with a black dot) of the local airfoil coordinate system, $C_{1/2}$, is located in the middle of the chord. Its position with respect to the blade root coordinate system is defined with x_{mb}-, y_{mb}- and z_{mb}-distances. The local airfoil coordinate system, $C_{1/2}$, is a right hand Cartesian coordinate system where:

- The x_{c2}-axis points towards the leading edge of the airfoil.
- The y_{c2}-axis is perpendicular to the chord and points towards the suction side of the airfoil.
- The z_{c2}-axis is perpendicular to the airfoil cross-section and points along the blade curved centerline towards the blade tip.
- The rotation of the local airfoil coordinate system, $C_{1/2}$, around the pitch z_{b}-axis is indicated by the local aerodynamic twist angle, Θ_{twist}. The positive direction is indicated with an arrow pointing upwind, from the plane created by the x_{b}- and z_{b}-axis of the blade root coordinate system, towards the chord.

The local airfoil elastic coordinate system is centered at the elastic center (marked with a red dot). Its position with respect to the local airfoil coordinate system, $C_{1/2}$, is defined with x_{e}-, and y_{e}-distances. It is a right hand Cartesian coordinate system where:

- The local structural twist angle, Θ_{Z}, between the chord line and the x_{ec}-axis defines the orientation of the local airfoil elastic coordinate system axes. The positive direction of Θ_{Z} is indicated with an arrow pointing towards the suction side of the airfoil.
- The y_{ec}-axis is perpendicular to the x_{ec}-axis.
- The z_{ec}-axis is perpendicular to the cross-section plane of the airfoil and points towards the blade tip.

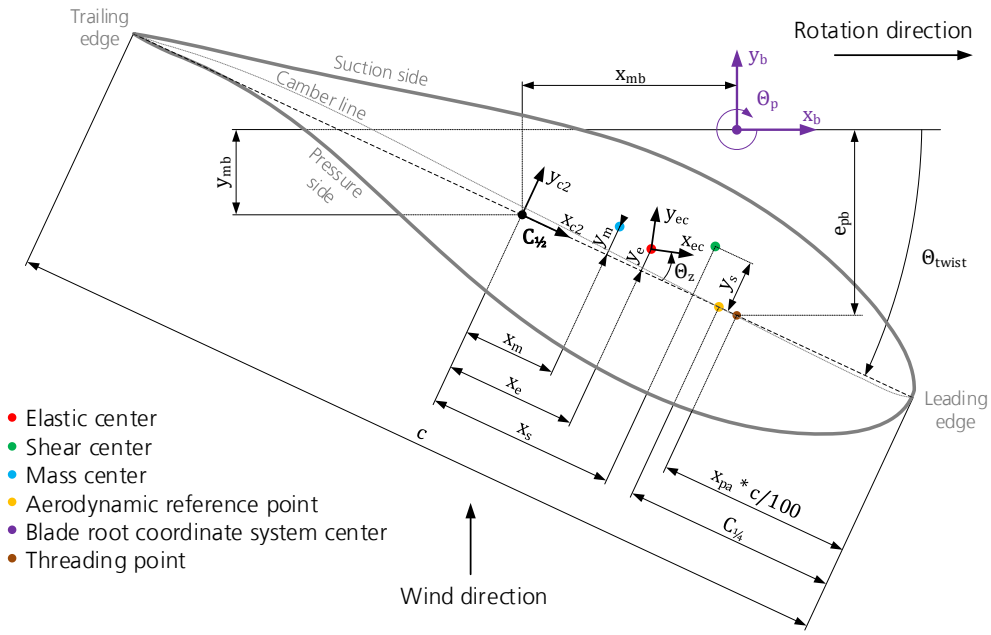

Figure 2-4: Local airfoil coordinate systems

Definitions of various centers within the airfoil cross-section:

- **Elastic center**: The point in the airfoil cross-section where an axial force (in the z_{ec}-direction) does not contribute to bending around the x_{ec}- or y_{ec}-axis but to pure axial strain. The elastic center is located at the intersection point of the principal bending axes x_{ec} and y_{ec}. In this document, the curve connecting the elastic centers of all cross sections is called the elastic axis.[1]
- **Shear center**: The point in the airfoil cross-section where the application of a shear force results in pure bending without any beam twist (no torsion).
- **Mass center**: The point where the center of mass of the airfoil cross-section is located.
- **Aerodynamic reference point**: The point in the airfoil cross-section where the lift, drag, and pitching moment coefficients of the respective airfoil are defined.[2] For slender profiles, the aerodynamic reference point is usually set at 25% of the chord length as shown in Figure 2-4, but for thicker profiles, this is not always the case.
- **Threading point:** In case of a blade without the pre-bend and the pre-sweep, the threading line coincides with the pitch axis. For the IWT-7.5-164, the threading line is curved with the pre-bend function with respect to the z_b-pitch axis.

[1] Sometimes this curve is also called the neutral axis, while some authors define the elastic axis as the curve connecting all shear centers. However, this is not the sense to be used in this document.

[2] This point is often called the aerodynamic center of the profile, but as the reference point does not necessarily coincide with the aerodynamic center, this term is not used in this document.

2.5
Blade centerline vs. blade pitch axis

Figure 2-5 shows the straight blade pitch z_b-axis and the curved centerline of the blade, passing through the $C_{1/2}$-centers of the airfoils. The structural blade properties are defined at the distances measured along the curved centerline of the blade, whereas geometrical properties are provided at the distances measured along the blade pitch z_b-axis.

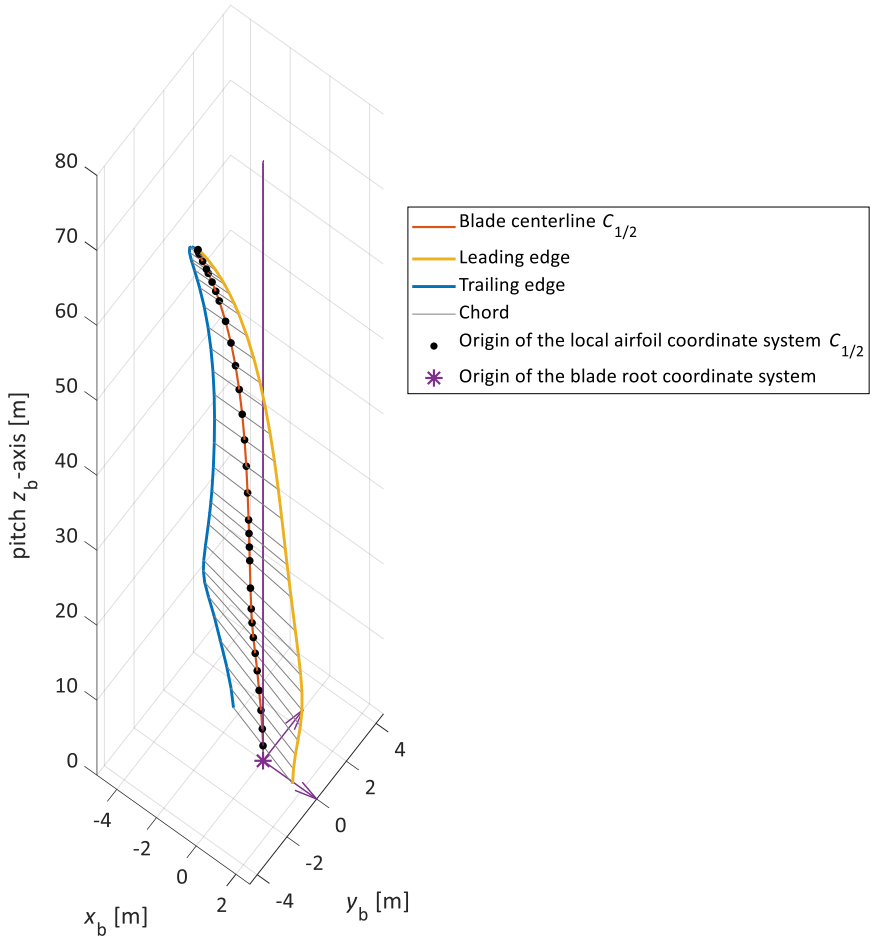

Figure 2-5: Blade centerline vs. blade pitch z_b-axis presented in blade root coordinate system

3
Wind turbine model definition

The goal was to design a large state-of-the-art upwind 3-bladed turbine with a relatively low rated power per swept area, a direct drive generator and a load-optimized control strategy and blade design. In order to facilitate comparability with industry turbines, the IWES Wind Turbine IWT-7.5-164 is designed according to the wind class IEC A1 [4]. Although sites with wind class A1 are rare, these conditions have been chosen to include the worst-case scenarios in terms of turbulence and extreme wind speeds. Table 3-1 summarizes the main parameters of the IWT-7.5-164 turbine.

Table 3-1: Summary of main turbine properties

Variable	Value	Unit	Description
P_r	7542	kW	Generator rated electrical power including losses
D_RN	163.44	m	Nominal rotor diameter (unconed blades)
D_R	163.34	m	Rotor diameter with coned blades
R_H	2	m	Hub radius
l_BC	79.98	m	Arc length of the blade, measured along the blade centerline. (In the blade definition, the last 2 cm are omitted, because the tip itself is a point without aerodynamic or structural features.)
l_B	79.72	m	Blade length along the pitch z_b-axis
V_in	3	m/s	Cut-in wind speed
V_r	11.7	m/s	Rated wind speed
V_out	25	m/s	Cut-out wind speed
$V_\mathrm{tip,r}$	85.53	m/s	Rated tip speed
Ω_min	5	rpm	The minimum rotational speed of the rotor when the generator is switched on
Ω_r	10	rpm	Rated rotational speed of the rotor
λ_r	7.31	-	Rated tip speed ratio
C_a	0.8	-	Nacelle aerodynamic drag coefficient
θ_cone	2	°	Blade cone angle in the upwind direction, measured between the unconed rotor plane and the pitch z_b-axis
θ_tilt	5	°	Shaft tilt angle upwards from the horizontal plane
m_RNA	536.78	t	Mass of rotor-nacelle assembly
m_B	30.93	t	Single blade mass
ψ_r	360	W/m²	Specific power per rotor swept area
η_tot	95	%	Total (combined mechanical and electrical) turbine efficiency

3.1 Rotor-nacelle assembly

Mass, centers of gravity (CG) and moments of inertia for different components of the rotor-nacelle assembly (RNA) are listed in Table 3-2, Table 3-3 and Table 3-4, respectively. Figure 3-1 shows the basic geometry of the RNA and positions of different CGs.

Table 3-2: Mass breakdown of RNA components

Component		Mass [t]	Description
Nacelle		250.00	Mass includes main bearings, main frame, nacelle housing, yaw drive, yaw bearing, internal systems
Rotor	Hub	104.00	Mass includes hub casting, pitch bearings, pitch system, spinner
	3 Blades	92.78	-
Generator	Rotor	60.30	-
	Stator	29.70	-
Total RNA		**536.78**	Summary of all masses

Table 3-3: Centers of gravity for nacelle, generator, and hub in tower top coordinate system, as shown in Figure 3-1

Component	Coordinates of CG [m]	Description
Nacelle	$x_t = 1.5$	Downwind from tower vertical axis
	$y_t = 0$	At tower vertical axis
	$z_t = 3.05$	Vertical from tower top plane
Generator	$x_t = 0$	At tower vertical axis
	$y_t = 0$	At tower vertical axis
	$z_t = 4 - 6.2 \sin(\theta_{tilt}) \approx 3.46$	Vertical from tower top plane
Hub	$x_t = - 6.2 \cos(\theta_{tilt}) \approx - 6.18$	Upwind from tower vertical axis
	$y_t = 0$	At tower vertical axis
	$z_t = 4$	Vertical from tower top plane

Table 3-4: Moment of inertia of nacelle, hub, and generator

Component		I [kg m²]	Description
Nacelle		2.48E+6	Rolling inertia (side-to-side) about nacelle CG
		7.19E+6	Yaw inertia about tower central z_t-axis at nacelle CG
		7.05E+6	Nodding inertia (fore-aft) about nacelle CG
Generator	Stator	2.57E+5	About tilted shaft axis at generator CG
		1.51E+5	Perpendicular to rotating shaft axis at generator CG
		1.51E+5	Perpendicular to rotating shaft axis at generator CG
	Rotor	5.22E+5	About tilted shaft axis at generator CG
		3.06E+5	Perpendicular to rotating shaft axis at generator CG
		3.06E+5	Perpendicular to rotating shaft axis at generator CG
Hub		3.74E+5	About tilted shaft axis at hub CG
		-	Perpendicular to rotating shaft axis at hub CG
		-	Perpendicular to rotating shaft axis at hub CG

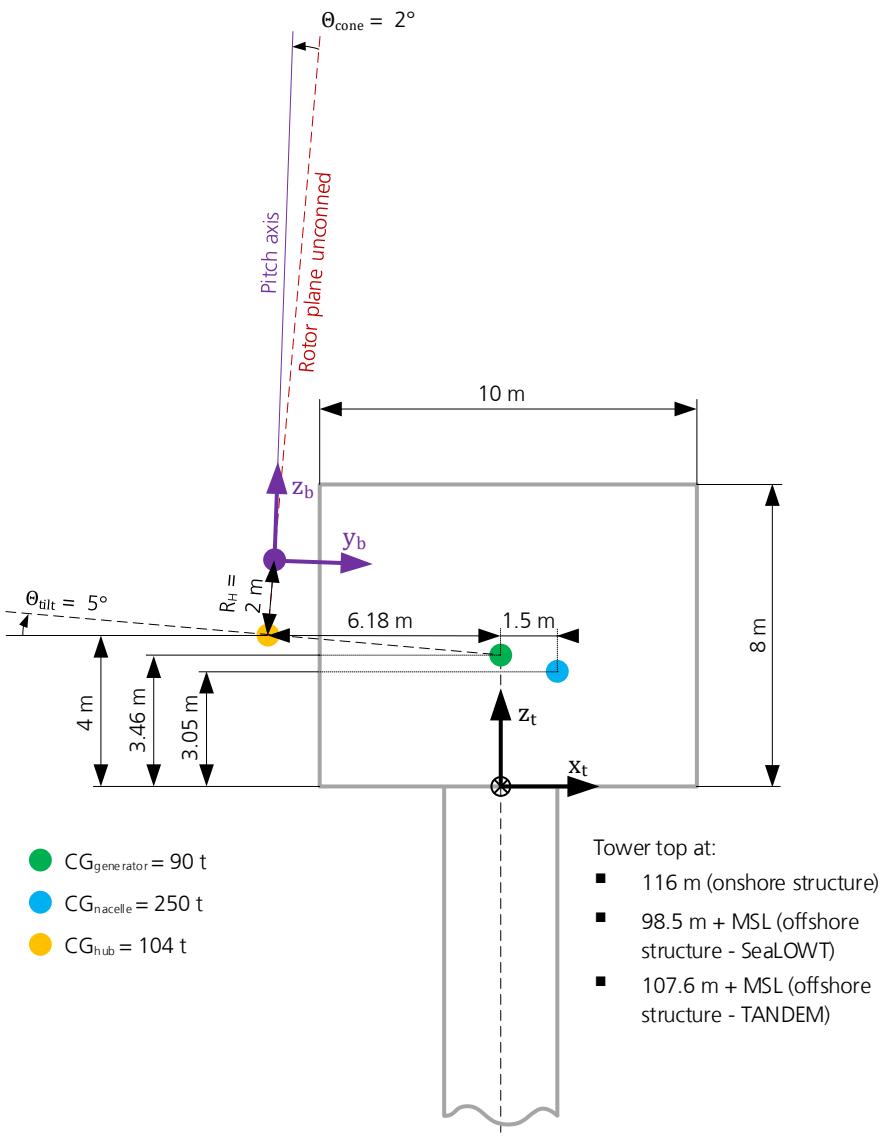

Figure 3-1: Schematic sketch of RNA geometry and centers of gravity positions

A supplementary information concerning the design of the nacelle housings and the spinner is presented in Appendix C. Note that this information is not crucial for the setup of the aeroelastic models of the IWT-7.5-164 turbine.

3.1.1 Blade

The blade model described in this section is based on a three-dimensional blade design. In this 3D blade design, the structure was designed according to GL guideline [5] based on selected design load cases from IEC [4]. For the fatigue analysis, the maximum strain approach [5] was applied. The stability of the spar cap region was design-driving, which resulted in a lightweight split spar cap concept rather than a continuous spar cap concept [6]. The 3D blade design was subsequently transformed into a beam model by calculating the stiffness and mass matrices of specific cross-sections.

In this section, the structural, geometrical and aerodynamic designs of the blade in terms of the beam model are described. General blade properties are listed in Table 3-5. Pre-bending in the flapwise direction is applied to increase the tower clearance.

Table 3-5: General blade properties

Variable	Value	Unit	Description
l_{BC}	79.98	m	Arc length of the blade, measured along the blade centerline (Note, that in the blade definition, the last 2 cm are omitted, because the tip itself is a point without aerodynamic or structural features)
$e_{\mathrm{pb,tip}}$	- 4.5	m	Blade pre-bend at the blade tip, measured along y_{b}-axis
λ_{r}	7.31	-	Rated tip speed ratio
m_{B}	30.93	t	Single blade mass

3.1.1.1 Structural properties

The structural properties of the blade were derived from BECAS [7] at 84 discrete positions measured from the center of the blade root coordinate system along the curved centerline of the blade, as shown in Figure 2-5.

The structural properties are plotted in Figure 3-2 to Figure 3-10. Their descriptions are provided in Table 3-6. They are defined with respect to the local airfoil coordinate system, which is centered at the half chord length $C_{1/2}$ of each airfoil, as shown in Figure 2-4.

The numerical values of the majority structural properties can be found in the Excel file, in the spreadsheet called "BECAS - structural data" under the following hyperlink (please refer to the Introduction section for more information on how to use the relative links):

IWT-7.5-164 - Blade definition

The Excel file automatically converts and interpolates structural properties from the BECAS coordinate system to the coordinate systems of three aeroelastic tools: Bladed, HAWC2, and the IWES in-house tool MoWiT (Modelica for Wind Turbines). The local airfoil coordinate systems of these tools are visualized in the respective Excel sheets. The

conversion and interpolation of data can be done for an arbitrary number of discrete positions.

The full 6x6 stiffness and mass matrices are also available, for $C_{1/2}$ and the threading[1] point as reference points, in BECAS_2D.out files. The files can be found under the following hyperlinks (please refer to the Introduction section for more information on how to use the relative links):

- Stiffness and mass matrices w.r.t $C_{1/2}$-centers (see Figure 2-4).
- Stiffness and mass matrices w.r.t threading points (see Figure 2-4).

Table 3-6: Description of structural variables

Variable	Unit	Description
r	m	Curved length distance from the center of the blade root coordinate system to $C_{1/2}$-centers of the local airfoil coordinate systems, measured along the blade centerline, as shown in Figure 2-5
x_{e}	m	Distance from the $C_{1/2}$-center to the elastic center, measured along the x_{c2}-axis, as shown in Figure 2-4
y_{e}	m	Distance from the $C_{1/2}$-center to the elastic center, measured along the y_{c2}-axis, as shown in Figure 2-4
x_{m}	m	Distance from the $C_{1/2}$-center to the mass center, measured along the x_{c2}-axis, as shown in Figure 2-4
y_{m}	m	Distance from the $C_{1/2}$-center to the mass center, measured along the y_{c2}-axis, as shown in Figure 2-4
x_{s}	m	Distance from the $C_{1/2}$-center to the shear center, measured along the x_{c2}-axis, as shown in Figure 2-4
y_{s}	m	Distance from the $C_{1/2}$-center to the shear center, measured along the y_{c2}-axis, as shown in Figure 2-4
r_{ix}	m	Radius of gyration w.r.t. rotation about principal bending x_{ec}-axis
r_{iy}	m	Radius of gyration w.r.t. rotation about principal bending y_{ec}-axis
A	m²	Cross-sectional area of the airfoil
I_{x}	m⁴	Area moment of inertia about principal bending x_{ec}-axis
I_{y}	m⁴	Area moment of inertia about principal bending y_{ec}-axis
K	m⁴/rad	Torsional stiffness constant about z_{ec}-axis. For a circular section, it is identical to the polar moment of inertia
m	kg/m	Mass per unit length
k_{x}	-	Shear factor in principal bending x_{ec}-direction
k_{y}	-	Shear factor in principal bending y_{ec}-direction
θ_{Z}	°	Local structural twist angle, measured between the x_{c2}-axis and the main principal bending x_{ec}-axis, as shown in Figure 2-4
G	N/m²	Shear modulus
E	N/m²	Young's modulus

[1] In case of a blade without the pre-bend and the pre-sweep, the threading line coincides with the pitch axis. For the IWT-7.5-164, the threading line is curved with the pre-bend function with respect to the z_{b}-pitch axis.

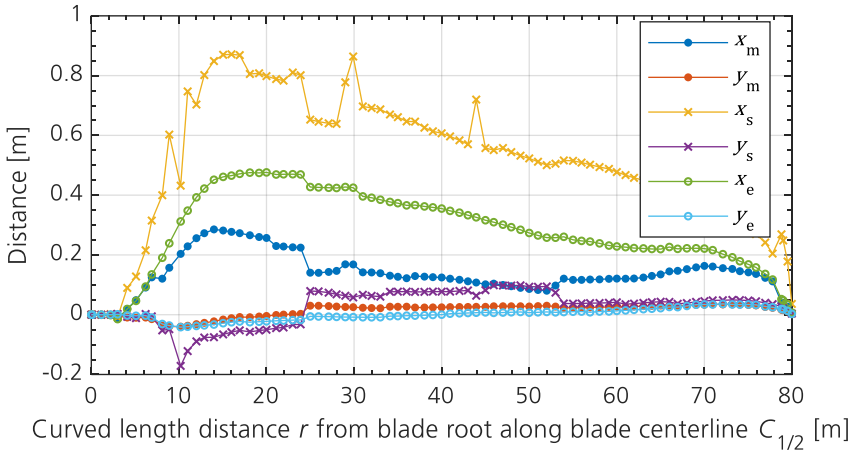

Figure 3-2: x_m, y_m distances to mass center; x_s, y_s distances to shear center; x_e, y_e distances to elastic center – all in local airfoil coordinate system

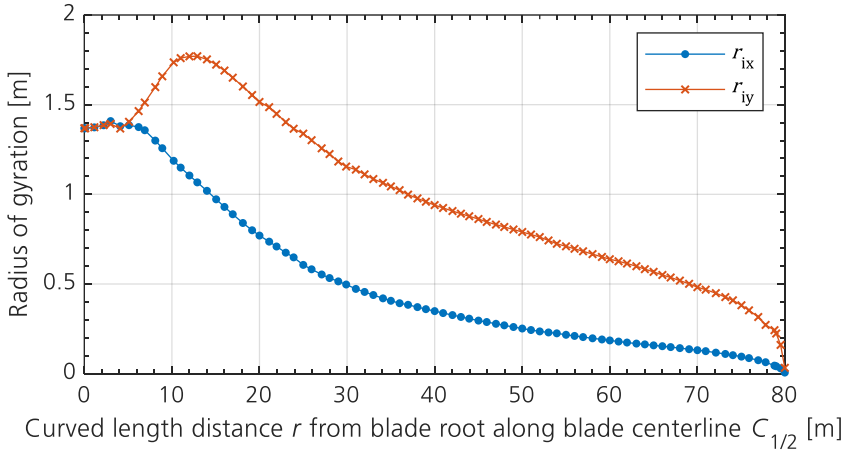

Figure 3-3: Radius of gyration r_{ix} and r_{iy} with respect to rotations about principal bending x_{ec}- and y_{ec}-axis

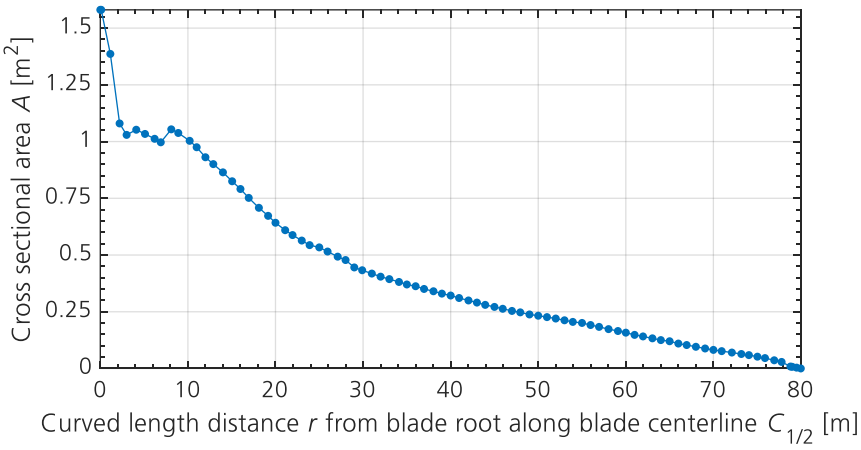

Figure 3-4: Cross-sectional area A of airfoil

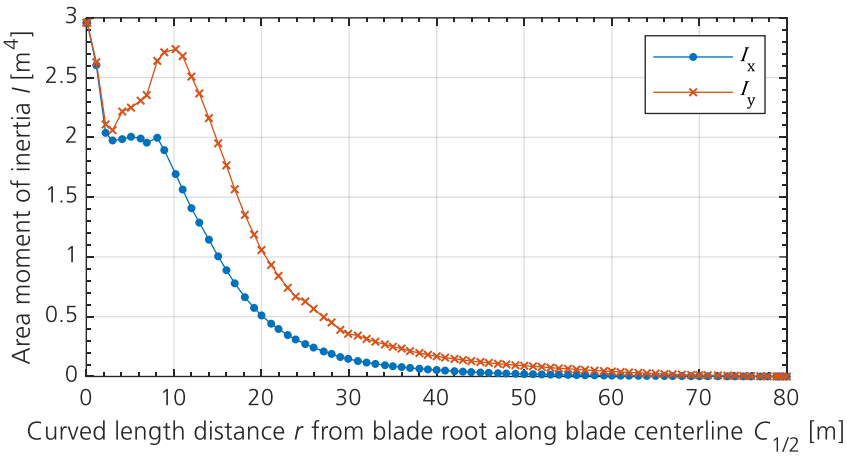

Figure 3-5: Area moments of inertia I_x and I_y about principal bending x_{ec}- and y_{ec}-axis

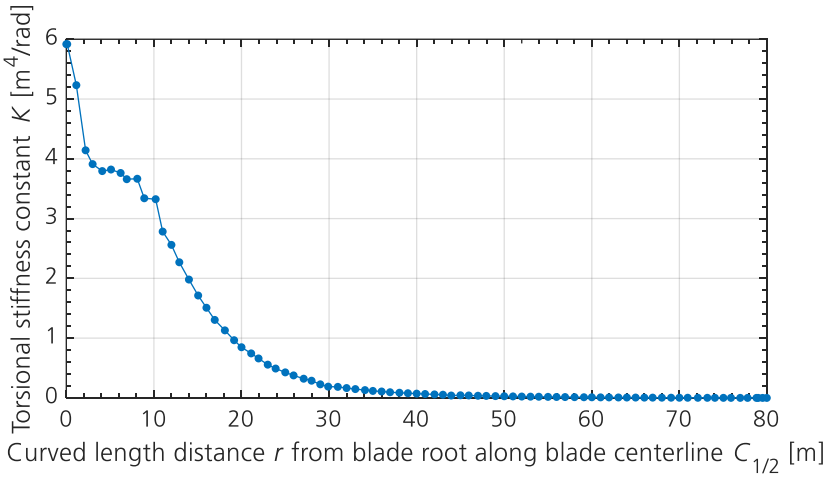

Figure 3-6: Torsional stiffness constant K about z_{ec}-axis

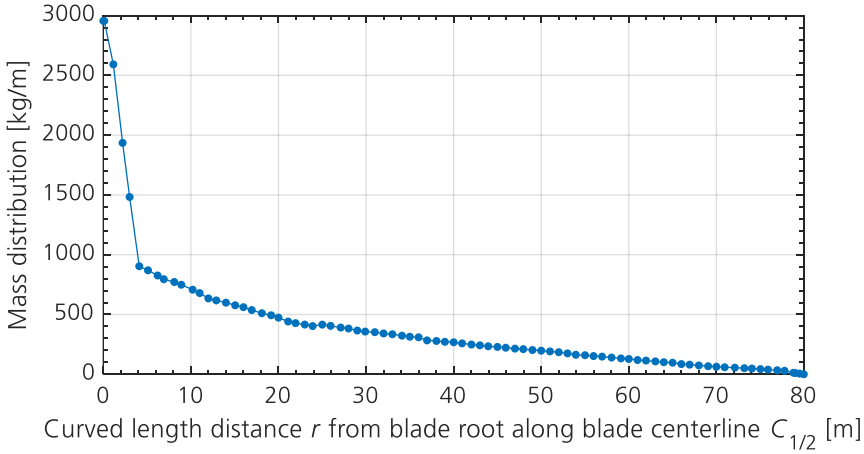

Figure 3-7: Mass distribution per unit length

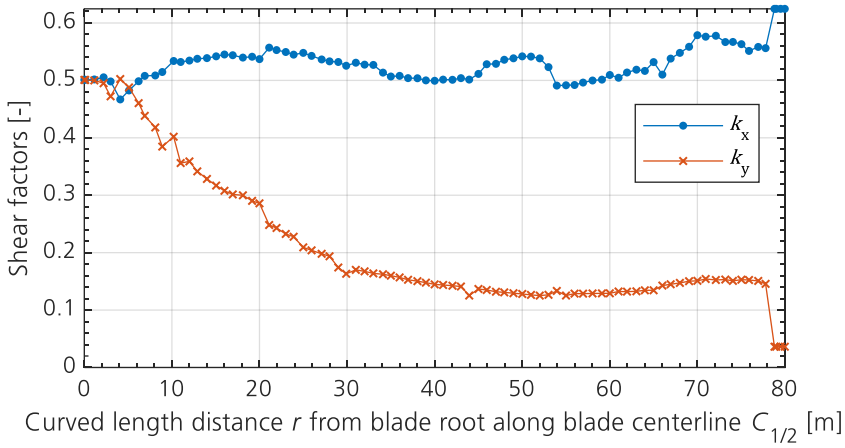

Figure 3-8: Shear factors k_x and k_y in principal bending x_{ec}- and y_{ec}-axis

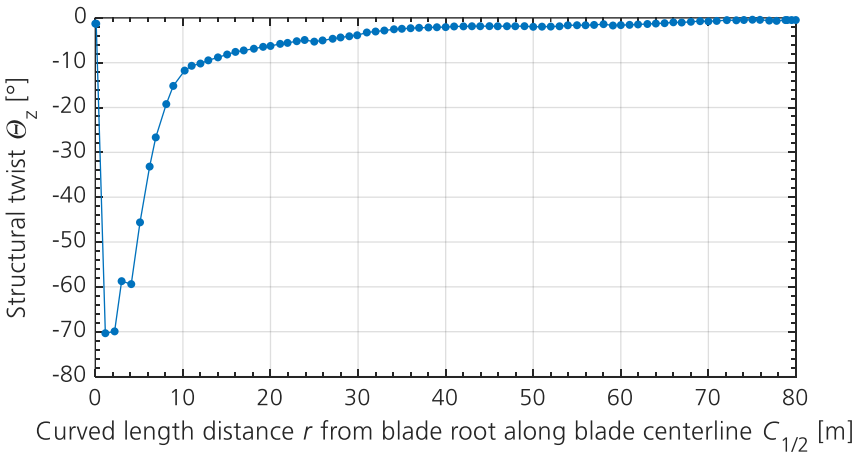

Figure 3-9: Local structural twist angle θ_Z between x_{c2}-axis and main principal bending x_{ec}-axis

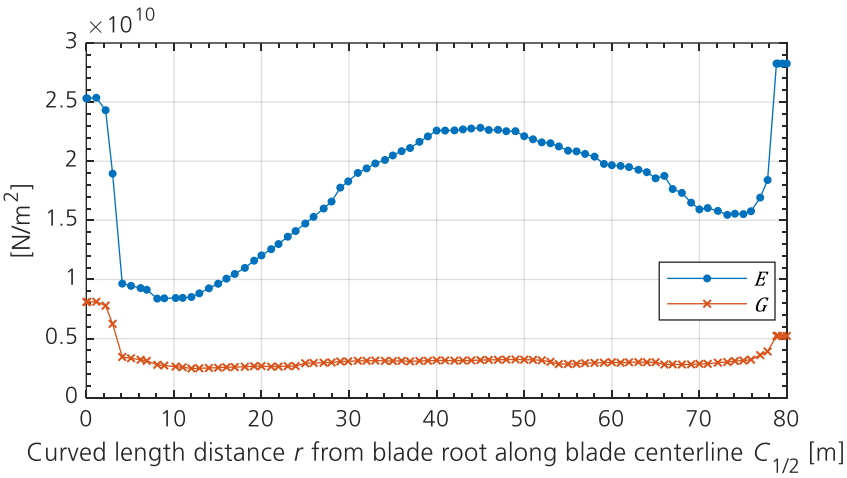

Figure 3-10: Shear modulus G and Young's modulus E

3.1.1.2 Geometrical properties

The geometrical properties of the blade were modeled with a spline-based, in-house aerodynamic tool. The tool generates a continuous geometry model, based on turbine parameters, the baseline airfoils (shape and polars) and the blade length. From this model, 75 discrete positions, measured from the center of the blade root coordinate system along the blade pitch z_b-axis, were derived, as shown in Figure 2-5.

The blade geometry is specified in terms of the blade centerline coordinates, the chord length, twist angle, relative thickness, alignment position, and pre-bend distributions. The description of the blade geometrical properties is listed in Table 3-7. The distribution of these properties along the blade pitch z_b-axis is plotted in Figure 3-11 to Figure 3-13.

Table 3-7: Description of blade geometrical properties

Variable	Unit	Description
x_{mb}	m	Distance from the center of the blade root coordinate system to the $C_{1/2}$-center of the local airfoil coordinate system, measured along the x_b-axis, as shown in Figure 2-4
y_{mb}	m	Distance from the center of the blade root coordinate system to the $C_{1/2}$-center of the local airfoil coordinate system, measured along the y_b-axis, as shown in Figure 2-4
z_{mb}	m	Distance from the center of the blade root coordinate system to the $C_{1/2}$-center of the local airfoil coordinate system, measured along the pitch z_b-axis
c	m	Chord length, distance between the leading and trailing edges, as shown in Figure 2-4
e_{pb}	m	Pre-bending from the pitch z_b-axis to the chord line, measured along the y_b-axis, as shown in Figure 2-4. This definition is correct, as long the pre-sweep is zero
θ_{twist}	°	Local aerodynamic twist angle between the plane, created by x_b- and z_b-axis of the blade root coordinate system, and the chord, positive in the upwind direction, as shown in Figure 2-4
t/c	%	Blade thickness ratio, defined as the largest distance between the suction side and the pressure side of the airfoil on a line perpendicular to the camber line, to the chord length
x_{pa}	%	Distance from the airfoil leading edge to the pitch z_b-axis, divided by the chord length, measured along the x_{c2}-axis, as shown in Figure 2-4

The numerical values of all geometrical properties can be found in the Excel file, in the spreadsheet called "Geometry" under the following link (please refer to the Introduction section for more information on how to use the relative links):

IWT-7.5-164 - Blade definition

The Excel file also automatically converts and interpolates geometrical properties to the coordinate systems of three aeroelastic tools: Bladed, HAWC2, and MoWiT. The local airfoil coordinate systems of these tools are visualized in the respective Excel sheets.

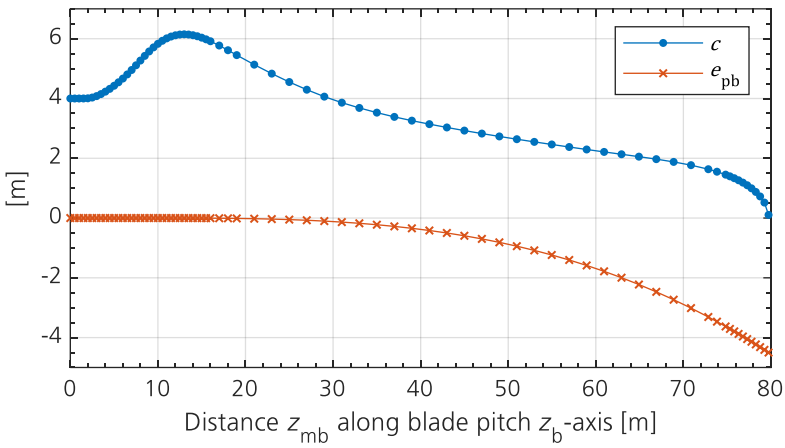

Figure 3-11: Chord length c and pre-bend e_{pb}

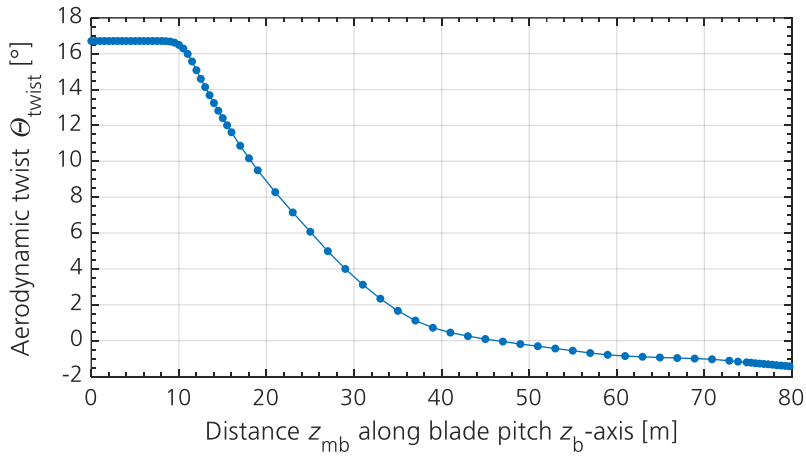

Figure 3-12: Local aerodynamic twist angle θ_{twist}

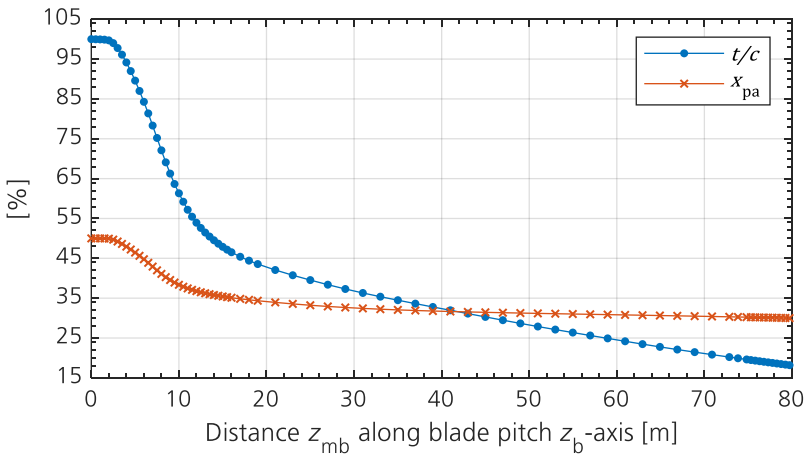

Figure 3-13: Relative thickness t/c and x_{pa}-distance

3.1.1.3
Aerodynamic properties

The aerodynamic design of the blade relies on two different families of airfoils:

- For the inner part of the blade, where the relative thickness exceeds the 35% threshold, three baseline airfoils developed at Fraunhofer IWES are considered [8], [9].
- For the outer part of the blade, where the relative thickness is equal or below the 35% threshold, four baseline airfoils developed at the TU Delft are considered [10], [11].

The relative thicknesses of the baseline airfoils and their spanwise locations are given in Table 3-8. The discretization of the entire blade geometry is achieved by generation of the so-called "blended" airfoil shapes, which are obtained by the linear interpolation of the two neighbor baseline airfoils, weighted by the relative spanwise distance.

The lift, drag and pitching moment aerodynamic coefficients for the baseline, as well as the blended airfoil shapes, are available in the Aerodynamic properties folder (please refer to the Introduction section for more information on how to use the relative links). These quantities are computed in RFOIL, a viscid-inviscid-interactive panel code coupled with integral boundary-layer equation [12], then corrected for the rotational effects and extrapolated for the angles of attack from -180° to 180°.

The operating conditions, for which the results have been obtained, are described in the following spreadsheet (please refer to the Introduction section for more information on how to use the relative links):

Polars

A detailed discussion of the procedure behind the generation of the aerodynamic data is available in Appendix A.

Table 3-8: Relative thickness and position along pitch z_{mb}-axis of baseline airfoils

Airfoil Name	t/c	z_{mb}
	-	m
Circle	1.00	0.00
IWES-A1 600-180	0.60	10.33
IWES-A1 500-100	0.50	13.76
IWES-A1 400-050	0.40	24.25
DU 00-W2-350	0.35	34.80
DU 91-W2-250	0.25	58.60
DU 08-W-210-6.5	0.21	70.47
DU 08-W-180-6.5	0.18	79.98

3.1.2
Performance coefficients

The aerodynamic coefficients for power, thrust and torque are presented in Figure 3-14 to Figure 3-16. The curves were generated with the turbine models implemented in Bladed V4.9 (see Section 5.1), with the following settings:

- Steady-state simulations with BEM theory.
- Fully-flexibly turbine simulated with 7 blade modes and 9 support structure modes.
- The Prandtl tip loss correction activated.
- Aerodynamics skew wake correction model switched off.
- Aerodynamics dynamic stall model switched off. Steady lift, drag and moment coefficient curves were used instead.
- Aerodynamics dynamic wake model set to equilibrium wake.

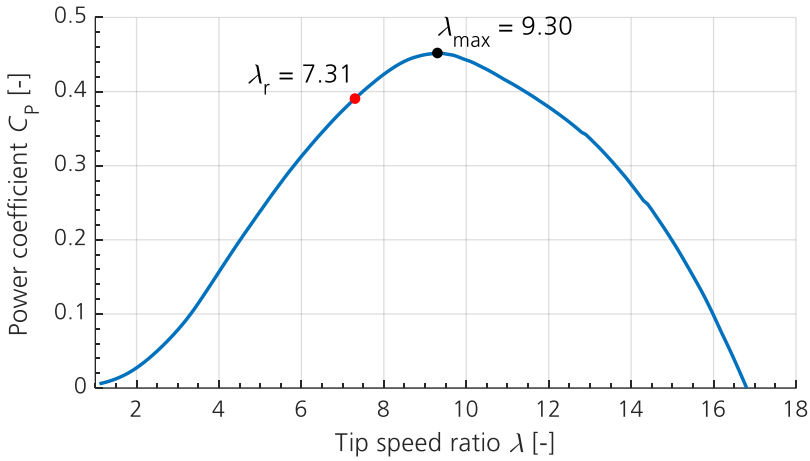

Figure 3-14: Power coefficient C_P as a function of tip speed ratio λ

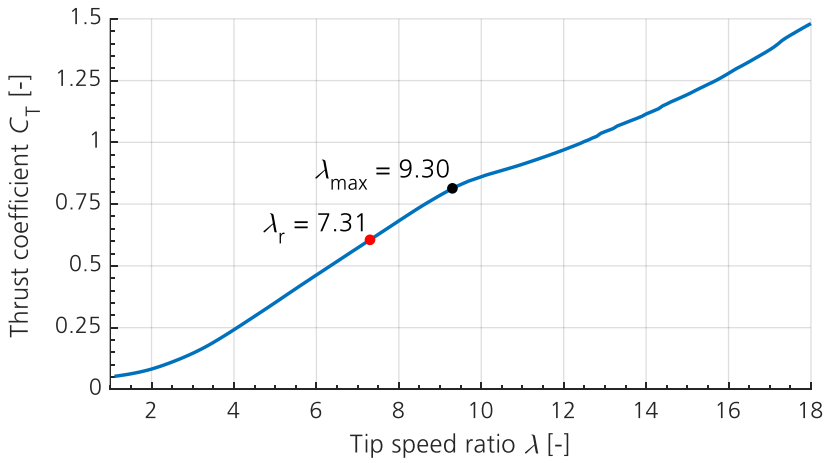

Figure 3-15: Thrust coefficient C_T as a function of tip speed ratio λ

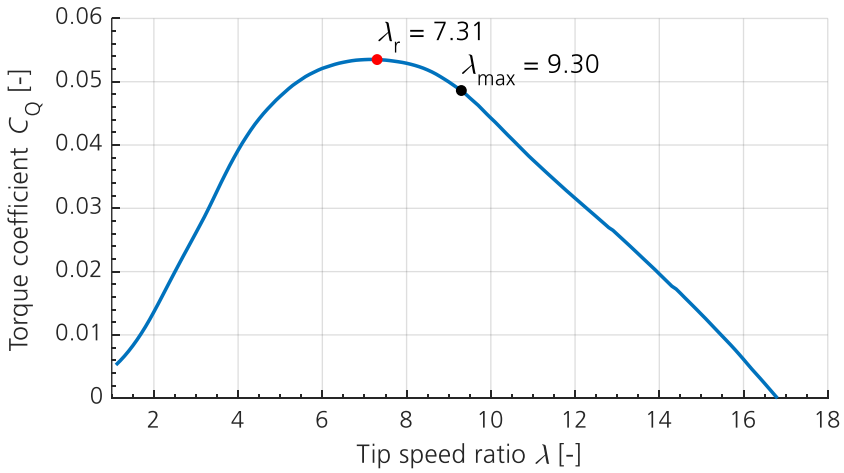

Figure 3-16: Torque coefficient C_Q as a function of tip speed ratio λ

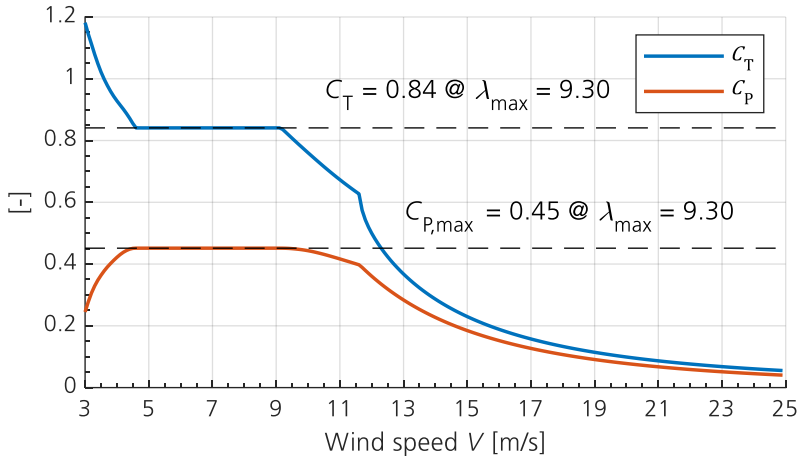

Figure 3-17: Power and thrust coefficients as a function of wind speed V

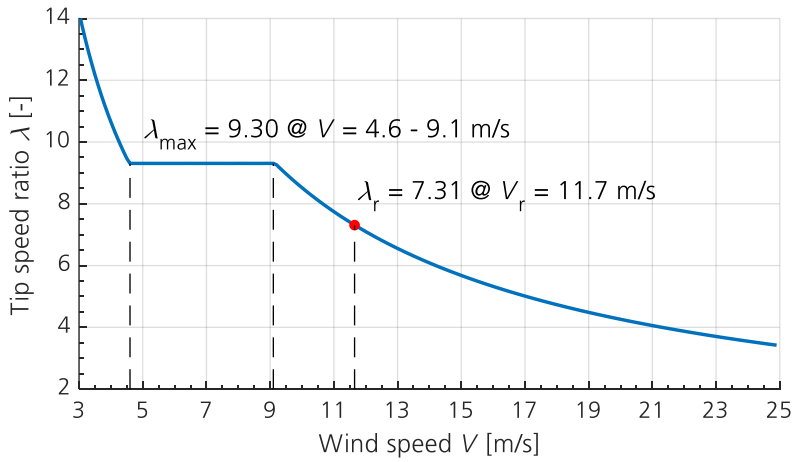

Figure 3-18: Tip speed ratio λ as a function of wind speed V

3.1.3
Steady-state performance

The steady state performance calculation was performed with turbine models implemented in Bladed V4.9 (see Section 5.1) with the following settings:

- Steady-state simulations with BEM theory.
- Uniform wind speed changing from V_{in} to V_{out}.
- The entire turbine was set as rigid.
- The Prandtl tip loss correction activated.
- The aerodynamics skew wake correction model and the dynamic stall model were switched off.
- The aerodynamics dynamic wake model was set to equilibrium wake.

The power, thrust and the pitch angle curves are shown in Figure 3-19, Figure 3-20, and Figure 3-21, respectively. Figure 3-22 shows the torque-speed-curve.

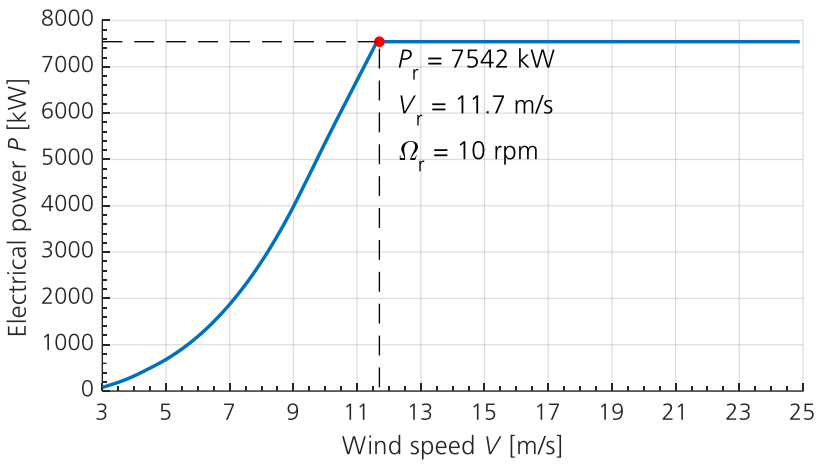

Figure 3-19: Power curve including losses

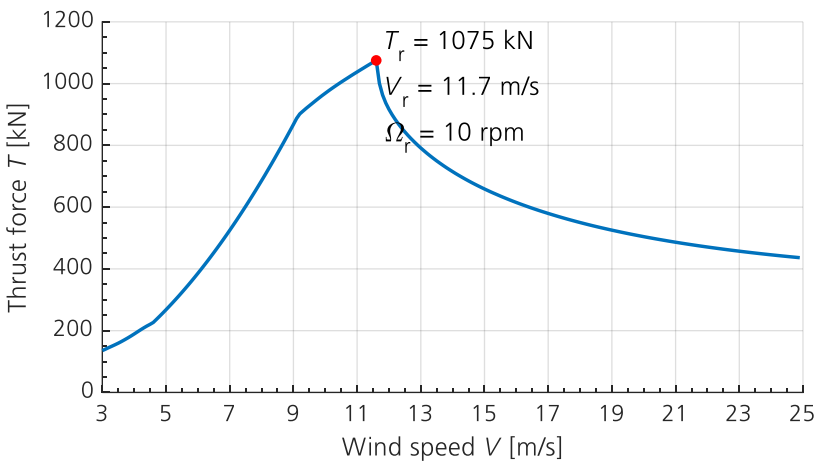

Figure 3-20: Thrust force T as a function of wind speed V

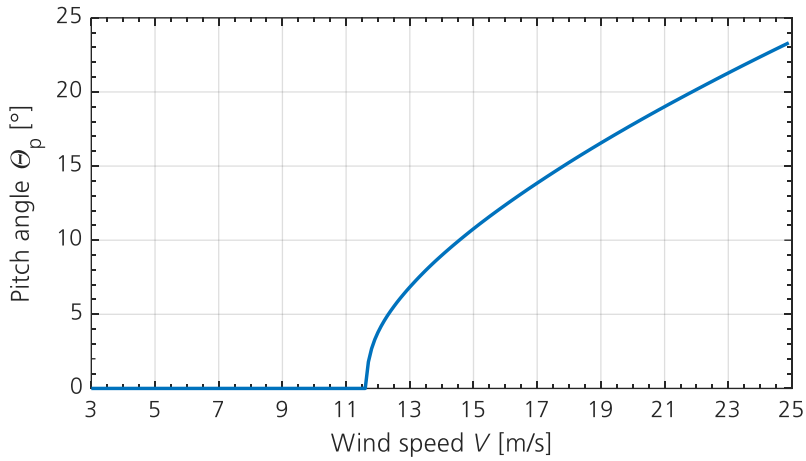

Figure 3-21: Pitch angle θ_P as a function of wind speed V

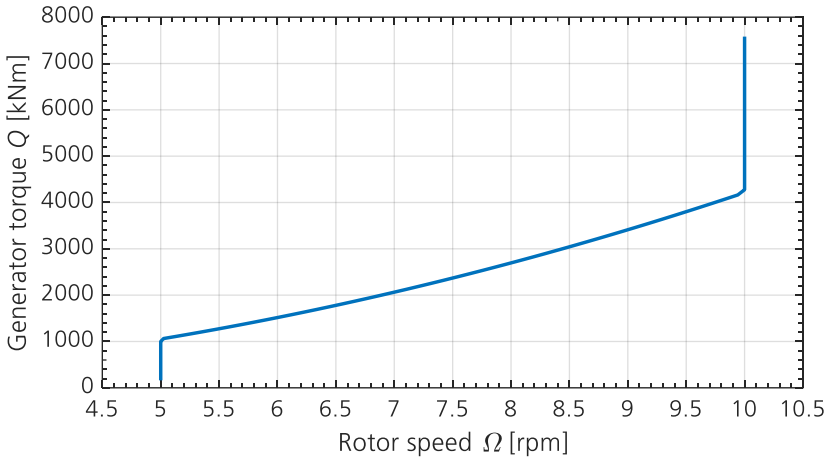

Figure 3-22: Generator torque Q as a function of rotor speed Ω

3.2 Onshore and offshore support structures

The IWT-7.5-164 turbine model is available with onshore and offshore monopile support structures. Their basic properties are presented in Table 3-9.

The onshore support structure consists of the concrete bottom part and the steel tower. This approach was also successfully used for the Multibrid M5000 prototype [13].

The offshore support structures are made of steel. They consist of the pile, transition piece, and the tower. They were designed by Ramboll within the SeaLOWT and TANDEM projects.

Table 3-9: Basic properties of monopile support structures

Property	Onshore	Offshore SeaLOWT	Offshore TANDEM
Mass	1467.4 t	1605.1 t	1589.4 t
Hub height	120 m	102.5 m above MSL	111.6 above MSL
Total height of the support structure	116 m	133.5 m	169.6
Mean sea level	-	35 m	30 m
Pile penetration depth into the seabed	-	32 m	32 m
Foundation model	rigid	6 DOFs stiffness matrix, which represents the part of the pile below seabed and the soil	6 DOFs stiffness matrix, which represents the part of the pile below seabed and the soil
First eigenfrequency including the influence of prescribed foundation model, and mass and inertia of the rigid RNA	0.254 Hz	0.216 Hz	0.226 Hz
Material	concrete/steel	steel	steel
Design concept	soft-stiff	soft-stiff	soft-stiff

Detailed structural and geometrical properties are available in the following Excel files (please refer to the Introduction section for more information on how to use the relative links):

- Onshore monopile support structure
- Offshore monopile support structure – SeaLOWT
- Offshore monopile support structure – TANDEM

3.3 Eigenfrequencies and Campbell diagram

Possible resonant vibrations of the turbine resulting from interaction with the spinning rotor are identified in the Campbell diagram, where the coupled system eigenfrequencies are plotted versus the rotational speed of the rotor. The inclined lines are multiples of 1P (rotor full revolution) and 3P (the tower passage of the blades) frequencies. The resonance may occur when the inclined lines intersect with the turbine eigenfrequencies. These frequencies usually do not have an ideal horizontal trend. They can vary depending on the rotor rotational speed and the associated centrifugal stiffening effect. They are also influenced by backward and forward whirling modes of the rotor and by the aerodynamic loads. The Campbell diagrams for the IWT-7.5-164 turbine model with onshore and offshore support structures are shown in Figure 3-23, Figure 3-24 (for the SeaLOWT monopile) and Figure 3-25 (for the TANDEM monopile). All three diagrams were derived from Bladed V4.9 models as presented in Section 5.1.

It should be noted that:

- The multiple blade coordinate transform [14] was used to ensure that the conversion from the rotating coordinate system of the blades and hub, to the stationary coordinate system of the tower, is done in the correct way. This procedure is required for the correct interpretation of the dynamic interaction between the rotation part (rotor) and the non-rotation part (support structure and nacelle).

- In case of a typical "soft-stiff" design approach for the bottom-fixed structures, the 1st fore-aft and side-to-side eigenfrequencies of the turbine should be located between the 1P and 3P frequencies of the permissible rotational speed of the rotor in order to avoid the excitation of these dominant modes.

- The 1P and 3P frequencies and the eigenfrequencies of the turbine should not be within ±5% of each other. In addition, the calculation uncertainties should be considered by including a safety margin of ±5% [15]. This leads to a total safety margin of 10%. The margin of more than 10% was achieved for the offshore support structures as shown in Figure 3-24 and Figure 3-25. In case of the onshore support structure, the 3P-excitation crosses the 1st eigenmode of the structure at the minimum rotational speed of 5 rpm (marked with red circle in Figure 3-23). However, the time domain simulations for the region around 5 rpm showed that the aerodynamic and structural damping will damp out possible excitations.

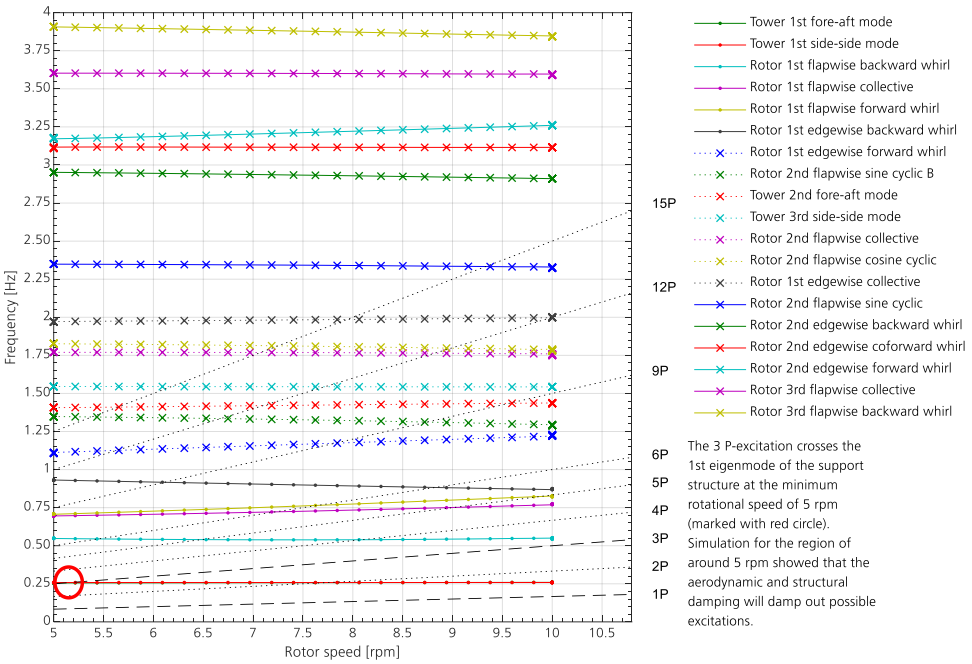

Figure 3-23: Campbell diagram for IWT-7.5-164 with onshore support structure for its entire operating region between cut-in and cut-out wind speeds

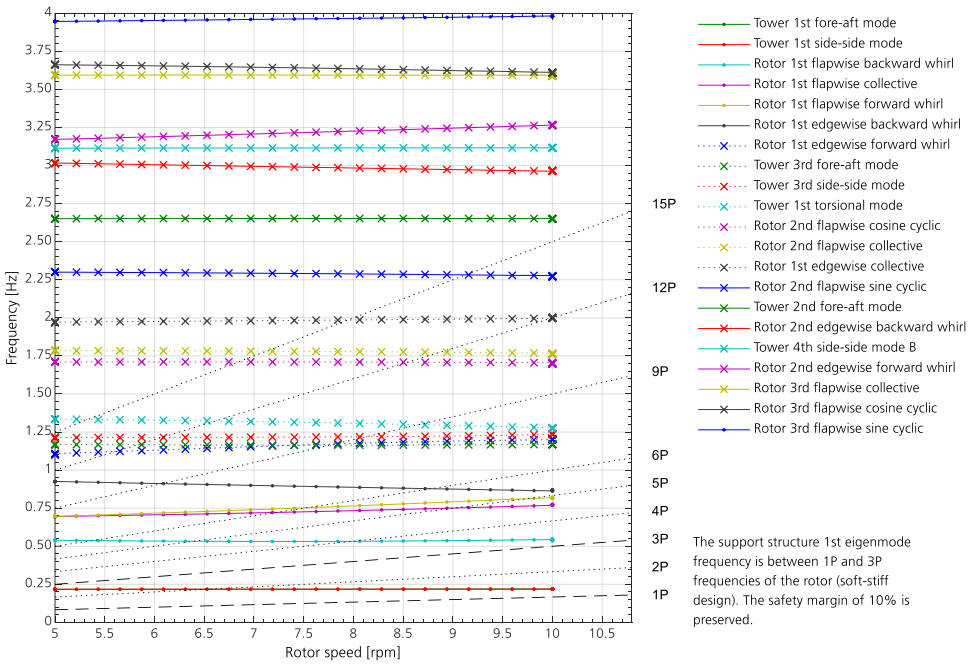

Figure 3-24: Campbell diagram for IWT-7.5-164 with SeaLOWT offshore support structure for its entire operating region between cut-in and cut-out wind speeds

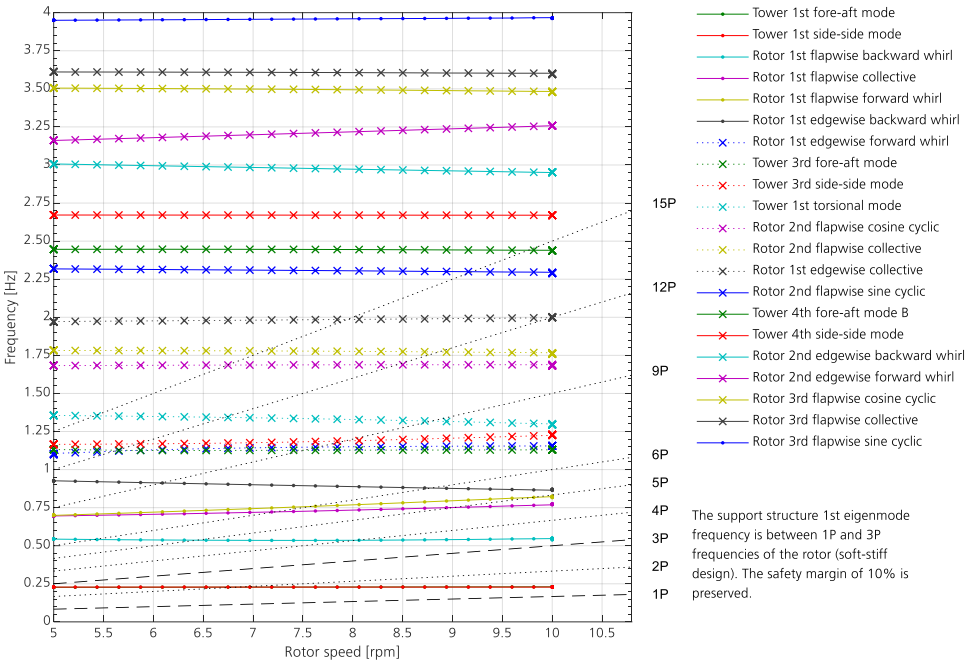

Figure 3-25: Campbell diagram for IWT-7.5-164 with TANDEM offshore support structure for its entire operating region between cut-in and cut-out wind speeds

4
Controller

The Bladed built-in controller is adapted for the IWT-7.5-164 turbine model implemented in Bladed V4.9.

The Basic DTU Wind Energy controller [16] [17] is adapted for the IWT-7.5-164 turbine model implemented in HAWC2.

It should be noted that these are two different controllers with different control settings. The controller highly influences turbine dynamics; therefore, the simulation results might not be comparable between these two models.

5
Numerical models of the IWT-7.5-164 turbine

This section describes the numerical models of the IWT-7.5-164 wind turbine. The models are implemented in two aeroelastic tools – Bladed V4.9 and HAWC2, and the MATLAB Simulink S-function exported from the in-house aeroelastic tool MoWiT. The models are available in the Aeroelastic models (please refer to the Introduction section for more information on how to use the relative links).

Table 5-1: Overview of the IWT-7.5-164 aeroelastic models

	Bladed V4.9	HAWC2	MATLAB Simulink S-function
Blade structural and geometrical properties	▪ Reduced set, derived at 32 discrete positions	▪ Full set consisting of 84 discrete positions for structural data and 75 discrete positions for geometrical data ▪ Reduced set, derived at 32 discrete positions	▪ Reduced set, derived for 31 members
Controller	Bladed built-in	Basic DTU Wind Energy controller	–
Onshore support structure	✓	✓	✓
Offshore support structures	✓	✗	✗

5.1
Bladed V4.9

The IWT-7.5-164 wind turbine with the onshore and offshore support structures is implemented in Bladed V4.9. Three numerical models are available under the following directory (please refer to the Introduction section for more information on how to use the relative links):

Bladed V4.9 models

It should be noted that all Bladed models:

- Are based on a reduced set of structural and geometrical blade properties redistributed at 32 discrete positions along the blade. This set of properties was derived and interpolated from the original data set (84 discrete positions for structural data and 75 discrete positions for geometrical data). All blade properties are available in the IWT-7.5-164 - Blade definition file (please refer to the Introduction section for more information on how to use the relative links).
- Are only provided with the Bladed built-in controller. The built-in controller was tuned using the automatic tuning procedure in Bladed.

5.2 HAWC2

The IWT-7.5-164 wind turbine with the onshore support structure is available under the following link (please refer to the Introduction section for more information on how to use the relative links):

HAWC2 model

It should be noted that the HAWC2 model:

- Can be used with both:
  - The full set of structural and geometrical blade properties (84 discrete positions for structural data, where the first section at r = 0.0 m is a copy of the data at r = 0.1 m calculated with BECAS; and 75 discrete positions for geometrical data).
  - The reduced set of structural and geometrical blade properties redistributed at 32 discrete positions along the blade. This set of properties was derived and interpolated from the full set of data All blade properties are available in the IWT-7.5-164 - Blade definition file (please refer to the Introduction section for more information on how to use the relative links).
- Is provided with the HAWC2 style DLL (Basic DTU Wind Energy controller with adapted properties).

5.3 MATLAB Simulink S-function

The IWT-7.5-164 wind turbine is modeled in Modelica, an equation-based and object-oriented modeling language, using the MoWiT library[1] developed at Fraunhofer IWES [18,19,20]. By means of the simulation environment, Dymola[2], this model can be compiled for Simulink as an S-function.

The IWT-7.5-164 wind turbine with the onshore support structure is available under the following link (please refer to the Introduction section for more information on how to use the relative links):

MATLAB Simulink S-function

It should be noted that the MATLAB Simulink S-function is based on a reduced set of structural and geometrical blade properties redistributed at 31 members along the blade. This set of properties was derived and interpolated from the original data set (83 discrete positions for structural data and 75 discrete positions for geometrical data). All blade

[1] formerly OneWind Modelica library
[2] https://www.3ds.com/products-services/catia/products/dymola/

properties are available in the IWT-7.5-164 - Blade definition file (please refer to the Introduction section for more information on how to use the relative links).

Furthermore, the MATLAB Simulink S-function does not include the wind turbine controller. Thus, the provided S-function serves as basis for Simulink users to develop their own control algorithms for a fully aeroelastic onshore wind turbine model.

5.3.1 Using the S-function

As the MATLAB Simulink S-function interacts with Dymola, the following steps have to be completed to ensure a correct setup of Simulink for integration of Dymola and to use the provided S-function in the next step.

1. Install MATLAB including Simulink. The provided S-function can be used for certain with MATLAB versions from R2012a (version 7.14) up to R2017a (version 9.2), as it was compiled with Dymola version 2018 FD01. It might work with newer MATLAB versions as well, but this is not guaranteed.

If the provided S-function should not only be simulated without the DymolaBlock GUI, but also the GUI should be used and for example, parameter values are to be changed, the following steps are required as well:

2. Install Dymola (there is no need to have a specific license, as only the installed folders are necessary). There is a free test version of Dymola available.
3. Set up MATLAB Simulink to work with Dymola:
   - Add the *Mfiles*-directory of Dymola and all of its sub-folders to the MATLAB path. Use the button "Set Path" in MATLAB to add the Dymola paths at the end of the MATLAB path list.
4. Ensure the correct setup of MATLAB:
   - Create a new Simulink (test) model. In the Simulink Library Browser look for the DymolaBlock library and check whether the DymolaBlock is available in Simulink.
   - If the DymolaBlock is not available, check if the Mfiles folders were imported successfully.

To import the provided MATLAB Simulink S-function, open a DymolaBlock in Simulink, double-click on the DymolaBlock and click on "Switch to generic import mode" in the lower right corner. Browse for the provided S-function file and load the S-function (button on the left), however, make sure that the checkbox for *omitting the description strings* is activated. Be careful with selecting the checkbox for generating results, as this will create a separate mat-file containing the simulation results, but will have a negative effect on the performance in Simulink.

5.3.2 Input parameters

For simulating the wind turbine model some inputs can be modified. The names and descriptions of the inputs and parameters are given in Table 5-2 and Table 5-3, respectively. Upon request, also other input parameters can be made available to be

modified in the MATLAB Simulink S-function. Furthermore, input signals for the controller are required to be provided, as the S-function of the wind turbine model is generated excluding the wind turbine controller. This way the user can implement, design, and tune his or her own controller for the IWT-7.5-164 wind turbine.

Table 5-2: Inputs for the MATLAB Simulink S-function

Within	Input	Unit	Description
	referencePitchAngle	rad	Demanded pitch angle for blades 1, 2, and 3
	referenceGeneratorTorque	Nm	Demanded generator torque, > 0
	Others (brakeSignal, pitchRate)	-	Other inputs to the S-function are not used and shall be zero

Table 5-3: Parameters for the MATLAB Simulink S-function

Within	Parameter[1]	Unit	Description
	initialRotorSpeed	rad/s	Initial rotor speed
rotor → param	initialAzimuthAngleBlade1	°	Initial azimuth angle for blade 1 [0 360]; zero indicates blade 1 pointing vertically up
nacelle → param	initialYawAngle	°	Initial nacelle yaw angle; zero would be main wind direction
operatingControl → param	initialPitchAngle	°	Initial pitch angle of blades (one scalar value for all three blades)
wind → param	vHub	m/s	Wind speed at hub height
	constDirectionAngle	°	Horizontal wind direction angle; positive indicates clockwise rotation of wind direction around *z*-axis in global coordinate system (Figure 2-1)
	constInclinationAngle	°	Vertical flow inclination angle; positive indicates rising

[1] Only available if DymolaBlock is installed (see 5.3.1).

5.3.3 Simulation outputs

The outputs of the MATLAB Simulink S-function are described in Table 5-4. Upon request, also other output signals can be included in the MATLAB Simulink S-function.

Table 5-4: Outputs from the MATLAB Simulink S-function

Output parameter	Unit	Description
HubWindSpeed	m/s	Free-stream wind speed at hub height in x-, y- and z-directions, according to the global coordinate system (Figure 2-1)
generatorPower	W	Generator rated electrical power including losses
generatorTorque	Nm	Generator torque without losses
generatorSpeed	rad/s	Generator speed
currentPitchAngle	rad	Pitch angles of blades 1, 2, and 3
azimuth	rad	Azimuth angle of blades 1, 2, and 3
bladeRootBending_Mx	Nm	In-plane bending moment at root of blades 1, 2, and 3, tilted, rotating, coned, not pitched, not twisted
bladeRootBending_My	Nm	Out-of-plane bending moment at root frame of blades 1, 2, and 3, tilted, rotating, coned, not pitched, not twisted
rotorSpeed	rad/s	Rotor rotational speed
rotorTorque	Nm	Aerodynamic rotor torque
rotorThrust	N	Aerodynamic rotor thrust
towerTop_displacements	m	Tower-top displacements in x-, y- and z-directions, according to the tower-top coordinate system (Figure 2-2)
towerTop_rotations	rad	Tower-top rotations around x-, y- and z-axes, according to the tower-top coordinate system (Figure 2-2)
towerTopAcc	m/s²	Tower-top accelerations in x-, y- and z-directions (in yawed frame) , according to the tower-top coordinate system (Figure 2-2)
yawBearing_bendingMoment_My	Nm	Tower top bending moment around y-axis, according to the tower-top coordinate system (Figure 2-2)
yawBearing_bendingMoment_Mz	Nm	Tower top bending moment around z-axis, according to the tower-top coordinate system (Figure 2-2)
towerBottom_bendingMoment_My	Nm	Tower bottom bending moment around y-axis, according to the global coordinate system (Figure 2-1)
towerBottom_bendingMoment_Mz	Nm	Tower bottom bending moment around z-axis, according to the global coordinate system (Figure 2-1)

Appendix A. Aerodynamic dataset

In this Appendix, the generation of the aerodynamic characteristics for both baseline and blended airfoil geometries along the blade is discussed. The final dataset is available in form of tabulated ASCII files, where the four columns report the angle of attack in degree, the lift, drag and pitching moment coefficients (please refer to the Introduction section for more information on how to use the relative links):

Polars

Different approaches are employed to determine the aerodynamic characteristics of the original airfoils:

- For the root circular section, the data are based on [21].
- For the IWES and TU Delft airfoils, the data are computed with RFOIL [12] in forced transition on the leading edge, i.e. at 1% of the chord length, without rotational correction.

The few inconsistencies arisen by the numerical simulation are fixed by means of a few script operations based on inputs derived by visual inspection.

The rotational effects are included as for the Snel-Houwink model [22].

The polar curves are then extrapolated up to the range limits of ±180°, by means of a combination of Viterna-Corrigan, flat-plate and reverse-flow model, as reported in [23], [24] and [25].

In Table A-1 a schematic view of the workflow employed is presented. The data provided within the companion material could be reproduced by means of:

- RFOIL, batch version 1.1.
- Python 2.7.

The extrapolated polar data could be exported to FAST, Bladed, and HAWC2, by means of auxiliary Python scripts, as reported schematically in Table A-2.

A detailed explanation of the companion material is available in the readme.

Table A-1: Workflow for generation of aerodynamic dataset

Aerodynamic dataset

Script-Name	Input(s)	Output(s)	Description
00a_run_orig_rot.py	RE_orig_rot.dat	Airfoils-Original/XX/rReY.pol	Compute polars between -25° and 25° with RFOIL in forced transition at 1% of chord length and Reynolds numbers belonging to rotational cases
00b_run_orig_sta.py	RE_orig_sta.dat	Airfoils-Original/XX/sReY.pol	Compute polars between -25° and 25° with RFOIL in forced transition at 1% of chord length and Reynolds numbers belonging to standstill cases
01a_fix_orig_rot.py	RE_orig_rot.dat Airfoils-Original/XX/rReY.pol	Airfoils-Original/XX/rReYfixed.pol	Fix not convergent points for rotational cases
01b_fix_orig_sta.py	RE_orig_sta.dat Airfoils-Original/XX/sReY.pol	Airfoils-Original/XX/sReYfixed.pol	Fix not convergent points for standstill cases
99a_repair_fix_rot.py	RE_orig_rot.dat Airfoils-Original/XX/rReYfixed.pol	Airfoils-Original/XX/rReYrepaired.pol	Repair unphysical behavior for rotational cases
99b_repair_fix_sta.py	RE_orig_sta.dat Airfoils-Original/XX/rReYrepaired.pol	Airfoils-Original/XX/sReYrepaired.pol	Repair unphysical behavior for standstill cases
02a_interp_fix_rot.py	RE_orig_rot.dat RE_rotating.dat Roshko.dat Airfoils-Original/XX/rReYrepaired.pol	Airfoils-Interpolated/XX/rReY.pol	Interpolation based on thickness and Reynolds number for rotational cases
02b_interp_fix_sta.py	RE_orig_sta.dat RE_standstill.dat Roshko.dat Airfoils-Original/XX/sReYrepaired.pol	Airfoils-Interpolated/XX/sReY.pol	Interpolation based on thickness and Reynolds number for standstill cases
03_correct_interp_rot.py	RE_rotating.dat geometry.dat cr.dat Airfoils-Interpolated/XX/rReY.pol	Airfoils-Corrected/XX/rReYsh.pol	Snel-Houwink correction for Himmelskamp effect [26] in rotational cases
04a_extrap_correct_rot.py	RE_rotating.dat geometry.dat Airfoils-Corrected/XX/rReYsh.pol		Extrapolation to -180° and 180° with a combination of Viterna-Corrigan, flat-plate and reversed flow model for the rotational cases
04b_extrap_interp_sta.py	RE_standstill.dat geometry.dat Airfoils-Interpolated/XX/sReY.pol		Extrapolation to -180° and 180° with a combination of Viterna-Corrigan, flat-plate and reversed flow model for the standstill cases

Table A-2: Workflow for export of aerodynamic dataset

Script-Name	Input(s)	Output(s)	Description
05a_export_AeroDyn13.py	RE_rotating.dat RE_standstill.dat Airfoils-Extrapolated/	export_AeroDyn13	Compute polars between -25° and 25° with RFOIL in forced transition at 1% of chord length and Reynolds numbers belonging to rotational cases
05b_export_AeroDyn15.py	RE_rotating.dat RE_standstill.dat Airfoils-Extrapolated/	export_AeroDyn15	Compute polars between -25° and 25° with RFOIL in forced transition at 1% of chord length and Reynolds numbers belonging to standstill cases
05c_export_BladedV4_7.py	geometry.dat RE_rotating.dat RE_standstill.dat Airfoils-Extrapolated/	export_BladedV4_7	Fix not convergent points for rotational cases
05d_export_HAWC2pc.py	geometry.dat Airfoils-Extrapolated/	export_HAWC2	Fix not convergent points for standstill cases

Aerodynamic dataset

Appendix B.
Aerodynamic characteristics of blended airfoils

In this Appendix, the aerodynamic characteristics and the geometrical description for the blended airfoils is presented. Different approaches are employed to determine the aerodynamic characteristics of the blended airfoils:

- For the stations 1-2, the data were based on literature sources.
- For the stations 3-6, the data were computed with RFOIL [22] in forced transition on the leading edge.
- The remaining airfoil coefficients were estimated via XFOIL [27] in forced transition on the leading edge.

The aerodynamic coefficients of the sections were determined for the Reynolds numbers given in Table B-1.

Table B-1: Reynolds numbers used for determination of airfoil coefficients

Station	Re [-]	Station	Re [-]
1	1.50E+06	17	7.50E+06
2	1.70E+06	18	7.60E+06
3	2.10E+06	19	7.70E+06
4	2.70E+06	20	7.80E+06
5	3.50E+06	21	7.80E+06
6	4.40E+06	22	7.80E+06
7	5.20E+06	23	7.70E+06
8	5.90E+06	24	7.60E+06
9	6.30E+06	25	7.40E+06
10	6.50E+06	26	7.20E+06
11	6.80E+06	27	6.80E+06
12	7.00E+06	28	6.60E+06
13	7.10E+06	29	5.80E+05
14	7.10E+06	30	4.40E+06
15	7.20E+06	31	4.80E+05
16	7.30E+06		

Appendix C.
Spinner and nacelle housing

The most wind turbine nacelles and hubs are covered by a housing to protect the components from weather conditions and increase the safety of personnel during maintenance, erection, etc.

Nacelle housing

The nacelle housing has a cuboid shape with rounded edges in the longitudinal direction and rounded edges at the front and back plate. The properties of the nacelle housing are given in Table C-1. The CG position is given w.r.t the origin of the coordinate system shown in Figure C-1, where the red axis shows the orientation in the x-direction, green in the y-direction, and blue in the z-direction.

Table C-1: Nacelle housing parameters

Parameter	Value	Unit
Nacelle housing width along x-axis	8	m
Nacelle housing height along y-axis	8	m
Nacelle housing length along z-axis	10	m
Housing wall thickness	0.02	m
CG x-coordinate	4	m
CG y-coordinate	4.311	m
CG z-coordinate	5.238	m
Nacelle housing volume	7.876	m^3
Area moment of inertia w.r.t. x-axis	169077	m^4
Area moment of inertia w.r.t. y-axis	178063	m^4
Area moment of inertia w.r.t. z-axis	140028	m^4
Material density	2000	kg/m^3
Nacelle housing weight	15751	kg

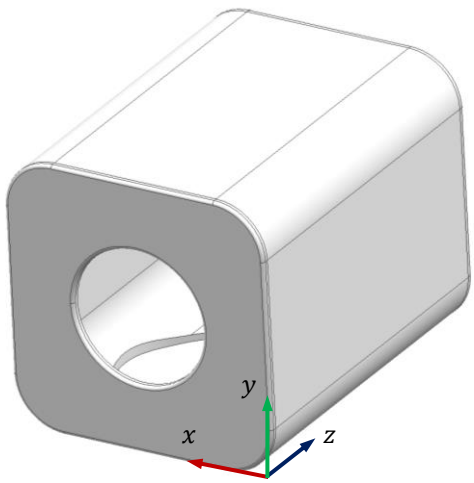

Figure C-1: Front view of nacelle housing

Spinner

The spinner has a half-ellipsoid shape. The properties of the spinner are given in Table C-2. The CG position is described from the origin of the coordinate system in Figure C-2 where the red axis shows the orientation in the x-direction, green in the y-direction, and blue in the z-direction.

Table C-2: Spinner parameters

Parameter	Value	Unit
Spinner diameter	8	m
Spinner length along y-axis	5.5	m
Wall thickness	0.02	m
CG x-coordinate	0.004	m
CG y-coordinate	2.975	m
CG z-coordinate	-0.020	m
Spinner volume	2.184	m^3
Area moment of inertia w.r.t. x-axis	17036	m^4
Area moment of inertia w.r.t. y-axis	21350	m^4
Area moment of inertia w.r.t. z-axis	17069	m^4
Material density	2000	kg/m^3
Spinner weight	4369	kg

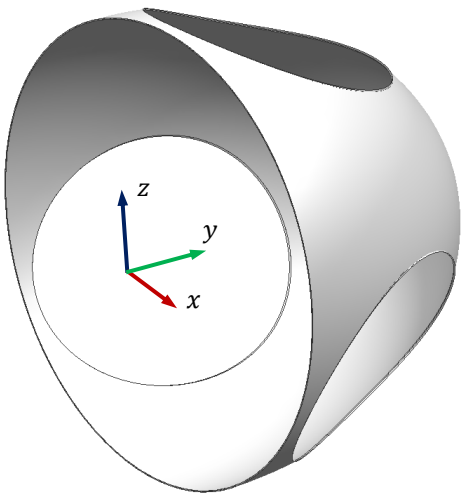

Figure C-2: Spinner

Bibliography

[1] J. Jonkmann, S. Butterfield, W. Musial, and G. Scott, "Definition of a 5-MW reference wind turbine for offshore system development," National Renewable Energy Laboratory, Golden, CO, NREL/TP-500-38060 2009. [Online]. http://www.nrel.gov/docs/fy09osti/38060.pdf

[2] Ch. Bak et al., "The DTU 10-MW reference wind turbine," Technical University of Denmark, Fredericia, Danish Wind Power Research 2013 2013. [Online]. http://orbit.dtu.dk/files/55645274/The_DTU_10MW_Reference_Turbine_Christian_Bak.pdf

[3] DNVGL, *DNVGL-ST-0437 Loads and site conditions for wind turbines*.: DNVGL, 2016. [Online]. https://rules.dnvgl.com/docs/pdf/DNVGL/ST/2016-11/DNVGL-ST-0437.pdf

[4] IEC, "IEC 61400-1 Edition 3 – Wind turbines – Part 1: Design requirements," International Electrotechnical Commission, Geneva, 2005.

[5] Germanischer Lloyd, "Guideline for the Certification of Wind Turbines," Germanischer Lloyd, Hamburg, 2010. [Online]. https://www.dnvgl.com/publications/certification-of-wind-turbines-98201

[6] M. Rosemeier and M. Bätge, "A concept study of a carbon spar cap design for a 80m wind turbine blade," *Journal of Physics: Conference Series*, vol. 524, pp. 1-7, 2014. [Online]. http://publica.fraunhofer.de/dokumente/N-301358.html

[7] J. P. A. A. Blasques, "User's Manual for BECAS: A cross section analysis tool for anisotropic and inhomogeneous beam sections of arbitrary geometry," Risø DTU – National Laboratory for Sustainable Energy, Roskilde, (Denmark. Forskningscenter Risoe. Risoe-R; No. 1785(EN)) ISSN 0106-2840, 2012. [Online]. http://orbit.dtu.dk/files/7711204/ris_r_1785.pdf

[8] L. Steer, "Design of thick flatback airfoils for wind turbine rotor blades," Ecole des Mines Paristech, European Master in Renewable Energy – EUREC, Thesis written at Fraunhofer IWES, Bremerhaven, MSc thesis 2013.

[9] L. Steer, M. Ahmad, R. Braun, B. Stoevesandt, and F. Sayer, "Influence of the trailing edge angle on the aerodynamic performance of thick flatback airfoils," in *Proceedings of EWEA*, Barcelona, 2014. [Online]. http://proceedings.ewea.org/annual2014/conference/posters/PO_215_EWEApresentation2014.pdf

[10] W. A. Timmer and R. P. J. O. M. van Rooij, "Summary of the Delft University wind turbine dedicated airfoils," *Journal of Solar Energy Engineering*, vol. 125, no. 4, pp. 488–496, November 2003. [Online]. http://solarenergyengineering.asmedigitalcollection.asme.org/article.aspx?articleid=1456892

[11] R. P. J. O. M. van Rooij and W. A. Timmer, "Roughness sensitivity considerations for thick rotor blade airfoils," *Journal of Solar Energy Engineering*, vol. 125, no. 4, pp. 468-478, November 2003. [Online]. http://lr.home.tudelft.nl/fileadmin/Faculteit/LR/Organisatie/Afdelingen_en_Leerstoelen/Afdeling_AEWE/Wind_Energy/Research/Publications/Publications_2003/doc/Rough_Airfoils_SOL_Vol125_RR2003.pdf

[12] H. Snel, R. Houwink, and J. Bosschers, "Sectional prediction of lift coefficients on rotating wind turbine blades in stall," Energy Research Centre of the Netherlands (ECN), Petten, ECN-C--93-052 1994.

[13] Multibrid Entwicklungsgesellschaft mbh, "Pressemitteilung Errichtung Multibrid m5000," Multibrid Entwicklungsgesellschaft mbh, Bremerhaven, 2004. [Online].

http://de.areva.com/areva-wind/liblocal/docs/News/Presse/Presse%202004/Pressemitteilung_Errichtung_M5000_191104.pdf

[14] R. P. Coleman and A. M. Feingold, "Theory of self-excited mechanical oscillations of helicopter rotors with hinged blade," National Advisory Committee for Aeronautics. Langley Aeronautical Lab., NACA Technical Report TR 1351 1958. [Online]. https://ntrs.nasa.gov/archive/nasa/casi.ntrs.nasa.gov/19930092339.pdf

[15] DIBt, "Richtlinie für Windenergieanlagen, Einwirkungen und Standsicherheitsnachweise," Deutsches Institut für Bautechnik, Berlin, 2012. [Online]. https://www.dibt.de/en/Departments/data/Aktuelles_Ref_I_1_Richtlinie_Windenergieanlagen_Okt_2012.pdf

[16] DTU Wind Energy. (2018) Basic DTU Wind Energy controller. [Online]. https://github.com/DTUWindEnergy/BasicDTUController

[17] M. H. Hansen and L. Ch. Henriksen, "Basic DTU Wind Energy controller," Roskilde, DTU Wind Energy E-0018 ISBN 978-87-92896-27-8, 2013. [Online]. http://orbit.dtu.dk/files/56263924/DTU_Wind_Energy_E_0028.pdf

[18] M. Leimeister and P. Thomas, "The OneWind® Modelica library for floating offshore wind turbine simulations with flexible structures," in *The 12th International Modelica Conference*, Prague, 2017, pp. 633-642. [Online]. http://www.ep.liu.se/ecp/132/070/ecp17132633.pdf

[19] P. Thomas, X. Gu, R. Samlaus, C. Hillmann, and U. Wihlfahrt, "The OneWind® Modelica library for wind turbine simulation with flexible structure - Modal reduction method in Modelica," in *The 10th International Modelica Conference*, Lund, 2014, pp. 939-948. [Online]. https://www.modelica.org/events/modelica2014/proceedings/html/submissions/ECP14096939_ThomasGuSamlausHillmannWihlfahrt.pdf

[20] M. Strobel et al., "The OnWind Modelica library for offshore wind turbines - Implementation and first results," in *The 8th International Modelica Conference*, Dresden, 2011. [Online]. http://www.ep.liu.se/ecp/063/067/ecp11063067.pdf

[21] A. Roshko, "Experiments on the flow past a circular cylinder at very high Reynolds number," Pasadena, CA, 1960. [Online]. https://authors.library.caltech.edu/10105/1/ROSjfm61.pdf

[22] B. O. G. Montgomerie Jensen, A. J. Brand, J. Bosschiers, and R. P. J. O. M. Van Rooji, "Three-dimensional effects in stall," Energy Research Centre of the Netherlands (ECN), Petten, ECN-C--96-079 1997. [Online]. https://www.ecn.nl/publications/ECN-C--96-079

[23] L. A. Viterna and R. D. Corrigan, "Fixed pitch rotor performance of large horizontal axis wind turbines," National Aeronautics and Space Administration. Lewis Research Center, Cleveland, OH, 1982. [Online]. https://ntrs.nasa.gov/archive/nasa/casi.ntrs.nasa.gov/19830010962.pdf

[24] J. L. Tangler and D. J. Kokurek, "Wind turbine post-stall airfoil performance characteristics guidelines for Blade-Element Momentum methods," National Renewable Energy Laboratory, Golden, CO, NREL/CP-500-36900 2004. [Online]. https://www.nrel.gov/docs/fy05osti/36900.pdf

[25] C. Lindenburg, "Stall coefficients: Aerodynamic airfoil coefficients at large angle of attack," ECN, ECN-RX–01-004 2001. [Online]. https://www.ecn.nl/publicaties/PdfFetch.aspx?nr=ECN-RX--01-004

[26] H. Himmelskamp, *Profile investigation on a rotating airscrew*. Göttingen, Germany, 1947, vol. 832 of Reports and translations / MAP Völenrode.

[27] M. Drela, "XFOIL: An analysis and design system for low Reynolds number airfoils," in *Low Reynolds Number Aerodynamics*, T. J. Mueller, Ed. Notre Dame, IN: Springer Berlin

Heidelberg, 1989, vol. 54, pp. 1–12. [Online].
http://link.springer.com/chapter/10.1007%2F978-3-642-84010-4_1